

# UC Berkeley

## SEMM Reports Series

### Title

Finite Element Formulations for Large Displacement and Large Strain Analysis

### Permalink

<https://escholarship.org/uc/item/0nv511hp>

### Authors

Bathe, Klaus-Jurgen

Ramm, Ekkehard

Wilson, Edward

### Publication Date

1973-09-01

500  
C23  
73-14

REPORT NO.  
UC SESM 73-14

STRUCTURES AND MATERIALS RESEARCH  
DEPARTMENT OF CIVIL ENGINEERING

---

---

# FINITE ELEMENT FORMULATIONS FOR LARGE DISPLACEMENT AND LARGE STRAIN ANALYSIS

by

KLAUS-JÜRGEN BATHE  
EKKEHARD RAMM  
EDWARD L. WILSON

---

---

SEPTEMBER 1973

STRUCTURAL ENGINEERING LABORATORY  
UNIVERSITY OF CALIFORNIA  
BERKELEY CALIFORNIA

EARTHQUAKE ENG. RES. CTR. LIBRARY  
Univ. of Calif. - 453 R.F.S.  
1301 So. 46th St.  
Richmond, CA 94804-4698 USA  
(510) 231-9403

---

Structures and Materials Research  
Department of Civil Engineering  
Division of Structural Engineering  
and Structural Mechanics

Report No. UCSESM 73-14

FINITE ELEMENT FORMULATIONS  
FOR LARGE DISPLACEMENT AND LARGE STRAIN ANALYSIS

by

Klaus-Jürgen Bathe

Ekkehard Ramm

Edward L. Wilson

Structural Engineering Laboratory  
University of California  
Berkeley, California

September 1973

EARTHQUAKE ENG. RES. CTR. LIBRARY  
Univ. of Calif. - 453 R.F.S.  
1301 So. 46th St.  
Richmond, CA 94804-4698 USA  
(510) 231-9403

---

## ABSTRACT

Starting from continuum mechanics principles, finite element incremental formulations for nonlinear static and dynamic analysis are reviewed and derived. No new formulation is presented. The aim in this report is a consistent summary, comparison, and evaluation of the two formulations, which are used in the general purpose nonlinear static and dynamic analysis program NONSAP. The general formulations include large displacements, large strains, material nonlinearities and nonconservative forces. For specific solutions in this report, elastic and hyperelastic materials only are considered.

The numerical solution of the continuum mechanics equations is achieved in NONSAP using isoparametric finite element discretization. The specific matrices which need be calculated in the formulations are discussed.

To demonstrate the applicability and the important differences in the formulations, the solution of static and dynamic problems involving large displacements and large strains are presented.

TABLE OF CONTENTS

	<u>Page</u>
ABSTRACT . . . . .	i
TABLE OF CONTENTS . . . . .	ii
ACKNOWLEDGEMENTS . . . . .	iv
NOTATION . . . . .	v
1. INTRODUCTION . . . . .	1
2. CONTINUUM MECHANICS FORMULATIONS . . . . .	5
2.1 Total Lagrangian Formulation . . . . .	8
2.2 Updated Lagrangian Formulation . . . . .	11
2.3 Linearization of Equilibrium Equations . . . . .	13
3. FINITE ELEMENT SOLUTION . . . . .	15
3.1 Finite Element Matrices . . . . .	15
3.2 Dynamic Analysis . . . . .	18
3.3 Equilibrium Iteration . . . . .	24
3.4 Constitutive Relations . . . . .	25
4. NONCONSERVATIVE LOADING . . . . .	29
5. SAMPLE SOLUTIONS . . . . .	31
1. Large Displacement Static Analysis of a Cantilever . . . . .	33
2. Large Displacement Static Analysis of a Shallow Arch . . . . .	36
3. Large Displacement Static Analysis of a Spherical Shell. . . . .	39
4. Large Strain and Large Displacement Static and Dynamic Analysis of Rubber Sheet with Hole . . . . .	41
5. Large Displacement Static Analysis of a Second Shallow Arch . . . . .	47
6. Dynamic Snap Buckling of a Shallow Arch . . . . .	50
6. COMPARISON OF TOTAL LAGRANGIAN AND UPDATED LAGRANGIAN FORMULATIONS . . . . .	54

TABLE OF CONTENTS (Cont.)

	<u>Page</u>
CONCLUSIONS . . . . .	58
REFERENCES . . . . .	59
APPENDIX A . . . . .	A1

## ACKNOWLEDGEMENTS

This research was performed by K.J. Bathe and E. Ramm in collaboration with E.L. Wilson.

The work of K.J. Bathe and E.L. Wilson was sponsored by the National Science Foundation, Grant GI-36387.

The work of E. Ramm was sponsored by the Deutsche Forschungsgemeinschaft, Grant Ra 218/1.

## NOTATION

All symbols are defined in the text. Important notation is also listed below. Components are referred to a Cartesian coordinate system;  $i, j, \dots = 1, 2, 3$ .

${}^m A$	=	Area of body in configuration $m$
${}^n C_{ijkl}$	=	Component of constitutive tensor referred to configuration $n$
${}^m \epsilon_{ij}$	=	Component of Green-Lagrange strain tensor using displacements from configuration $n$ to configuration $m$ and referred to configuration $n$
${}^m \epsilon_{ij} \equiv {}^m_m \epsilon_{ij}$	=	Component of Almansi strain tensor in configuration $m$
${}^n \epsilon_{ij}$	=	Component of strain increment tensor referred to configuration $n$
${}^n e_{ij}$	=	Linear part of strain increment ${}^n \epsilon_{ij}$
${}^n n_{ij}$	=	Nonlinear part of strain increment ${}^n \epsilon_{ij}$
${}^m f_i$	=	Component of body force vector per unit mass in configuration $m$ referred to configuration $n$
$h_k$	=	Finite element interpolation function associated with nodal point $k$
${}^m n_i$	=	Component of surface normal in configuration $m$
${}^m \rho$	=	Specific mass of body in configuration $m$
${}^m R$	=	Total external force applied in configuration $m$
${}^m S_{ij}$	=	Component of 2nd Piola-Kirchhoff stress tensor in configuration $m$ referred to configuration $n$
${}^n S_{ij}$	=	Component of stress increment in ${}^m S_{ij}$
${}^m \tau_{ij} \equiv {}^m_m \tau_{ij}$	=	Component of Cauchy stress tensor in configuration $m$
${}^m t_i$	=	Component of surface traction vector in configuration $m$ referred to configuration $n$
${}^m u_i$	=	Component of displacement vector from initial position to configuration $m$

- $u_i$  = Increment in displacement component  
 ${}^m u_i^k$  = Displacement component of nodal point k in configuration m  
 ${}^m_{n,i,j} u_i$  = Derivative of displacement component to configuration m with respect to coordinate  ${}^n x_j$   
 ${}^n u_{i,j}$  = Derivative of displacement increment with respect to coordinate  ${}^n x_j$   
 ${}^m V$  = Volume of body in configuration m  
 ${}^m x_i$  = Cartesian coordinate in configuration m  
 ${}^m x_i^k$  = Cartesian coordinate of nodal point k in configuration m  
 ${}^m_{n,i,j} x_i$  = Derivative of coordinate in configuration m with respect to coordinate  ${}^n x_j$

#### Matrices

- ${}^m_{n,B,L}$  = Linear strain displacement matrix in configuration m referred to configuration n  
 ${}^m_{n,B,NL}$  = Nonlinear strain displacement matrix in configuration m referred to configuration n  
 ${}^n C$  = Tangent material property matrix referred to configuration n  
 ${}^m_n F$  = Vector of nodal point forces in configuration m (n = 0 in T.L. formulation and n = m in U.L. formulation)  
 ${}^m_{n,K,L}$  = Linear strain stiffness matrix in configuration m referred to configuration n  
 ${}^m_{n,K,NL}$  = Nonlinear strain stiffness matrix (also called geometric or initial stress stiffness matrix) in configuration m referred to configuration n  
 $M$  = Mass matrix  
 ${}^m R$  = Vector of external loads in configuration m  
 ${}^m_{n,S,n}$  = 2nd Piola-Kirchhoff stress matrix and vector in configuration m and referred to configuration n

$m_T, m_T^*$  = Cauchy stress matrix and vector in configuration  $m$

$u$  = Vector of displacement increments from configuration 1 to configuration 2

## 1. INTRODUCTION

In nonlinear dynamic finite element analysis involving large displacements, large strains and material nonlinearities, it is necessary to resort to an incremental formulation of the equations of motion. Various formulations are used in practice (see references). Some procedures are general and others are restricted to account for material nonlinearities only, or for large displacements but not for large strains, or the formulation may only be applicable to certain types of elements. Limited results have been obtained in dynamic nonlinear analysis involving large displacements and large strains.

Currently, the general purpose nonlinear finite element analysis program NONSAP is being developed at the University of California, Berkeley [ 2]. An important aspect in the development of the program is to assess which general finite element formulation should be implemented.

In dynamic analysis numerical integration of the finite element equations of motion is required. Extensive research is currently being devoted towards the development of stable and accurate integration schemes [ 1] [ 3] [17] [26]. However, it need be realized that a proper evaluation and use of an integration method is only possible if a consistent nonlinear finite element formulation is used.

The earliest nonlinear finite element analyses were essentially based on extensions of linear analyses and have been developed for specific applications (for a comprehensive list of references, see the books by Oden [28] and Zienkiewicz [38]). The procedures were primarily developed on an intuitive basis in order to obtain solutions to the specific problems considered. However, to provide general

analysis capabilities using isoparametric (and related) elements a general formulation need be used. The isoparametric finite element discretization procedure has proven to be very effective in many applications, and lately it has been shown that general nonlinear formulations based on principles of continuum mechanics can efficiently be implemented.

Basically, two different approaches have been pursued in incremental nonlinear finite element analysis. In the first, static and kinematic variables are referred to an updated configuration in each load step. This procedure is generally called Eulerian, moving coordinate or updated formulation. Murray and Wilson [24], Felippa[7], Yaghmai and Popov [34] [35], Farhoomand [6] Sharifi and Popov [30], Yamada [36], Stricklin et al [33], Heifitz and Costantino [12], Belytschko and Hsieh [4] have presented some form of this formulation.

In the second approach, which is generally called Lagrangian formulation, all static and kinematic variables are referred to the initial configuration. This procedure is used by Oden [27] [28], Marcal [23], Hibbit et al [13], Larsen [19], McNamara [25], Sharifi and Yates [31], Stricklin et al [32] [33], Haug and Powell [10]. A survey paper of the Lagrangian formulation in static analysis was presented by Hibbit et al [13], where it is stated that additional research is required for use of an equivalently consistent updated formulation.

It is apparent that with the different formulations available, in the development of a general purpose nonlinear dynamic analysis program a decision need be made on the procedure to be used. An

important consideration is that using any formulation based on continuum mechanics principles, in which all nonlinear effects are included, the same results should be obtained in the analyses. Stricklin et al discussed a moving coordinate formulation and a Lagrangian formulation and pointed out that the latter is more general and computationally more efficient [33]. Yamada compared a Eulerian and Lagrangian formulation and predicted for a simple truss structure a maximum difference of about 25% in the displacements [36]. Dupuis et al analyzed arches using the Lagrangian and an updated formulation and also calculated a much different response by either formulation[5].

The purpose of this report is to present and compare in detail the two general formulations that are used in program NONSAP, and to show their general applicability in nonlinear static and dynamic analysis. The formulations are termed total Lagrangian and updated Lagrangian formulations and they are based on the work of the authors cited above. For specific solutions in this report, only elastic and hyperelastic materials are considered.

Both procedures are derived from the basic principle of virtual work and are valid for nonlinear material behavior, large displacements and large strains. It is pointed out that, in theory, there is no difference in the two formulations. Any difference in the numerical results arise from the fact that different descriptions of material behavior are assumed, and if the material constants are transformed appropriately, identical numerical results are obtained. Therefore, the question of which formulation should be used merely depends on the relative numerical effectiveness of the two methods. In the paper specific attention is directed to the

---

efficiency of either formulation.

To demonstrate the applicability and the important differences in the two formulations, the numerical operations required for solution are studied and a variety of sample solutions are presented. These include the large displacement and large strain static and dynamic analysis of a rubber-like material, the static and dynamic buckling of elastic arches and shells, and the large displacement analysis of a cantilever with conservative and nonconservative loading.

## 2. CONTINUUM MECHANICS FORMULATIONS

Consider the motion of the body in Fig. 1. The aim is to evaluate the equilibrium positions of the body at the discrete time points  $0, \Delta t, 2\Delta t, 3\Delta t, \dots$ , where  $\Delta t$  is an increment in time. Assume that the solution for the kinematic and static variables for all time steps from time = 0 to time =  $t$ , inclusive, have been solved for, and that the solution for time =  $t + \Delta t$  is required next. It is noted that the solution process for the next required equilibrium position is typical and would be applied repetitively until the complete solution path has been solved for. In the derivation of the equilibrium equations, reference is made to the initial (time = 0), current (time =  $t$ ) and next unknown (time =  $t + \Delta t$ ) configurations of the body, which are referred to as configurations "0", "1" and "2", respectively.

The motion of the body is considered in a fixed Cartesian coordinate system, Fig. 1, in which all kinematic and static variables are defined. The coordinates describing the configuration of the body at time = 0 are  ${}^0x_1, {}^0x_2, {}^0x_3$ , at time =  $t$  are  ${}^1x_1, {}^1x_2, {}^1x_3$ , and at time =  $t + \Delta t$  are  ${}^2x_1, {}^2x_2, {}^2x_3$ , where the superscript refers to the configuration of the body and the subscripts to the coordinate axes. The notation for the displacements of the body is similarly to the notation for the coordinates; at time =  $t$  the displacements are  ${}^1u_i, i = 1,2,3$  and at time =  $t + \Delta t$  the displacements are  ${}^2u_i, i = 1,2,3$ ; therefore

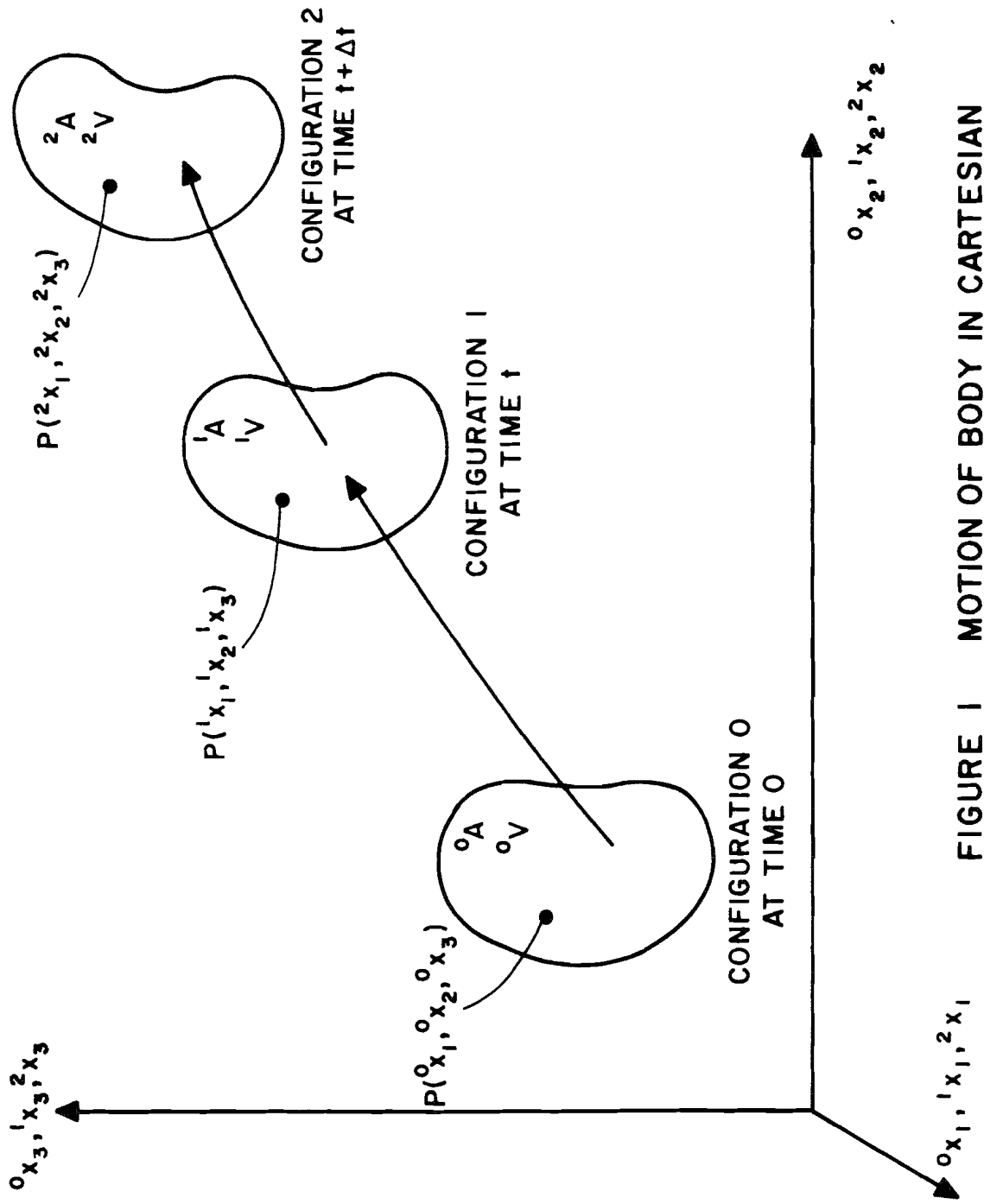


FIGURE 1 MOTION OF BODY IN CARTESIAN COORDINATE SYSTEM

$${}^k x_i = {}^o x_i + {}^k u_i \quad \begin{matrix} k = 1,2 \\ i = 1,2,3 \end{matrix}$$

The increments in the displacements from configurations 1 to 2 are denoted as

$$u_i = {}^2 u_i - {}^1 u_i \quad i = 1,2,3$$

The basic aim of the formulation is to establish an equation of virtual work from which the unknown static and kinematic variables in configuration 2 can be solved for. Using the principle of virtual displacements, because the isoparametric displacement based finite element procedure shall be employed for numerical solution, the equilibrium of the body in configuration 2 requires that [22],

$$\int_{{}^2 V} {}^2 \tau_{ij} \delta_2 e_{ij} {}^2 dv = \int_{{}^2 A} {}^2 t_k \delta u_k {}^2 da + \int_{{}^2 V} {}^2 \rho {}^2 f_k \delta u_k {}^2 dv \quad (1)$$

where  ${}^2 \tau_{ij}$  = Cartesian components of the Cauchy stress tensor, i.e. actual physical stresses referred to unit area in configuration 2,  ${}^2 t_k$  = surface force component,  ${}^2 f_k$  = body force component per unit mass,  ${}^2 \rho$  = mass density,  $\delta u_k$  = virtual variation in current displacement components and  $\delta_2 e_{ij}$  = the corresponding virtual variations in strains,  $\left( \delta_2 e_{ij} = \delta \frac{1}{2} ({}^2 u_{i,j} + {}^2 u_{j,i}) \right)$ . It should be noted that the  $\delta_2 e_{ij}$  are kinematic quantities which arise by transforming the right hand side of Eq. (1), and which are identified to be of the form of a variation of a small strain expression. In Eq. (1) and the equations to follow the summation convention of tensor notation is implied and the integrations are performed over the volume  ${}^2 V$  and area  ${}^2 A$  of the body. A left superscript

denotes the configuration in which the quantity occurs and a left subscript denotes the configuration with respect to which the quantity is measured. Noting that Cauchy stresses are always referred to the configuration in which they do occur, ( ${}^2\tau_{ij} \equiv {}^2\tau_{ij}$ ), in Eq. (1) all quantities exist and are measured with respect to configuration 2.

Equation (1) cannot be solved directly since the configuration 2 is unknown. An approximate solution can be obtained by referring all variables to a known previously calculated equilibrium configuration. For this purpose, in principle, any one of the already calculated equilibrium configurations could be used. In practice, however, the choice lies essentially between two different formulations, namely, the total Lagrangian formulation (T.L.) and the updated Lagrangian (U.L.) formulation which are presented in the following sections.

### 2.1 Total Lagrangian Formulation

The formulation called here total Lagrangian (T.L.) formulation is generally referred to as Lagrangian formulation and has been used a great deal in static analysis [11] [13] [23] [33].

In the formulation all variables in Eq. (1) are referred to the initial configuration 0 of the body. The applied forces in Eq. (1) are evaluated using

$${}^2t_k \, {}^2da = {}^0t_k \, {}^0da \quad ; \quad {}^2\rho \, {}^2f_k \, {}^2dv = {}^0\rho \, {}^0f_k \, {}^0dv \quad (2)$$

where it is assumed that the direction and magnitude of the forces  ${}^2t_k$  and  ${}^2f_k$  are independent of the configuration 2, i.e. conservative loading only is considered. Nonconservative loading conditions

are discussed in a later section.

The volume integral of Cauchy stresses times virtual variations in small strains in Eq. (1) can be transformed to give [22]

$$\int_V {}^2\tau_{ij} \delta {}^2e_{ij} {}^2dv = \int_V {}^2S_{ij} \delta {}^2\varepsilon_{ij} {}^0dv \quad (3)$$

where  ${}^2S_{ij}$  = Cartesian components of the 2nd Piola - Kirchhoff stress tensor corresponding to configuration 2 but measured in configuration 0, and  $\delta {}^2\varepsilon_{ij}$  = virtual variations in the Cartesian components of the Green - Lagrange strain tensor in configuration 2 referred to configuration 0,

$${}^2S_{ij} = \frac{{}^0\rho}{{}^2\rho} {}^0x_{i,s} {}^2\tau_{sr} {}^0x_{j,r} \quad (4)$$

$$\delta {}^2\varepsilon_{ij} = \delta \left( \frac{1}{2} ({}^2u_{i,j} + {}^2u_{j,i} + {}^2u_{k,i} {}^2u_{k,j}) \right) \quad (5)$$

A comma denotes differentiation with respect to the coordinate following, where the left subscript indicates the configuration in which the coordinate is measured, i.e. in Eq. (5) all differentiations are with respect to  ${}^0x_i$ ,  $i = 1,2,3$ . It need be noted that the integral of Piola - Kirchhoff stresses times virtual variations in the Green-Lagrange strains is defined over the initial configuration 0 of the body.

Substituting the relations in Eqs. (2) and (3) into Eq. (1), the following equilibrium equation of the body in configuration 2 but referred to configuration 0 is obtained,

$$\int_{o_V} {}^2S_{ij} \delta {}^2\varepsilon_{ij} {}^o dy = \int_{o_A} {}^2t_k \delta u_k {}^o da + \int_{o_V} {}^o \rho {}^2f_k \delta u_k {}^o dv \quad (6)$$

or

$$\int_{o_V} {}^2S_{ij} \delta {}^2\varepsilon_{ij} {}^o dv = {}^2R \quad (7)$$

where  ${}^2R$  is the total force applied in configuration 2.

Since the stresses  ${}^2S_{ij}$  and strains  ${}^2\varepsilon_{ij}$  are unknown, for

solution, the following incremental decompositions are used

$${}^2S_{ij} = {}^1S_{ij} + {}^o S_{ij} \quad (8)$$

$${}^2\varepsilon_{ij} = {}^1\varepsilon_{ij} + {}^o \varepsilon_{ij} \quad (9)$$

where  ${}^1S_{ij}$  and  ${}^1\varepsilon_{ij}$  are the known 2nd Piola - Kirchhoff stresses and Green-Lagrange strains in configuration 1. Using the displacement definition of the Green-Lagrange strain tensor, it follows from Eq. (9) that  $\delta {}^2\varepsilon_{ij} = \delta {}^o \varepsilon_{ij}$  and

$${}^o \varepsilon_{ij} = {}^o e_{ij} + {}^o n_{ij} \quad (10)$$

where

$${}^0e_{ij} = \frac{1}{2} \left( {}^0u_{i,j} + {}^0u_{j,i} + {}^1u_{k,i} {}^0u_{k,j} + {}^0u_{k,i} {}^1u_{k,j} \right) \quad (11)$$

$${}^0n_{ij} = \frac{1}{2} {}^0u_{k,i} {}^0u_{k,j} \quad (12)$$

The incremental 2nd Piola - Kirchhoff stresses  ${}^0S_{ij}$  are related to the incremental Green-Lagrange strains  ${}^0e_{ij}$  using the constitutive tensor  ${}^0C_{ijrs}$ , i.e.

$${}^0S_{ij} = {}^0C_{ijrs} {}^0e_{rs} \quad (13)$$

Equation (7) can now be written as

$$\begin{aligned} & \int_{{}^0V} {}^0C_{ijrs} {}^0e_{rs} \delta {}^0e_{ij} {}^0dv + \int_{{}^0V} {}^1S_{ij} \delta {}^0n_{ij} {}^0dv \\ & = {}^2R - \int_{{}^0V} {}^1S_{ij} \delta {}^0e_{ij} {}^0dv \end{aligned} \quad (14)$$

which represents a nonlinear equation for the incremental displacements  $u_i$ .

## 2.2 Updated Lagrangian Formulation

Most updated formulations previously used are approximate in that they are restricted to small strains or even constant strain

conditions within each finite element used for numerical solution [4][24]. However, Yaghmai introduced a general procedure, and the U.L. formulation given here is largely based on his work [34]. The use of the U.L. formulation in NONSAP was also presented in [2].

In the U.L. formulation all variables in Eq. (1) are referred to configuration 1, i.e. the updated configuration of the body. By an analogous procedure to the derivation in Section 2.1, Eq. (1) is in this case transformed to

$$\int_{1V} {}^2_1S_{ij} \delta_1^2 \epsilon_{ij} {}^1dv = {}^2R \quad (15)$$

where  ${}^2_1S_{ij}$  = Cartesian components of the 2nd Piola-Kirchhoff stress tensor and  ${}^2_1\epsilon_{ij}$  = Cartesian components of the Green-Lagrange strain tensor increment from configuration 1 to configuration 2 and referred to configuration 1. Since conservative loading is considered  ${}^2R$  is evaluated as in the T.L. formulation. The incremental stress decomposition used in this case is

$${}^2_1S_{ij} = {}^1\tau_{ij} + {}^1S_{ij} \quad (16)$$

where  ${}^1\tau_{ij}$  = Cauchy stresses and  ${}^1S_{ij}$  = 2nd Piola-Kirchhoff stress increments, referred to configuration 1. Considering the strain increments  ${}^2_1\epsilon_{ij}$ , the following relations hold

$${}^2_1\epsilon_{ij} = {}^1\epsilon_{ij} \quad (17)$$

$${}^1\epsilon_{ij} = {}^1e_{ij} + {}^1n_{ij} \quad (18)$$

where

$${}^1e_{ij} = \frac{1}{2} ({}^1u_{i,j} + {}^1u_{j,i}) \quad (19)$$

$${}^1n_{ij} = \frac{1}{2} ({}^1u_{k,i} - {}^1u_{k,j}) \quad (20)$$

The constitutive relation between stress and strain increments used now is

$${}^1S_{ij} = {}^1C_{ijrs} {}^1\epsilon_{rs} \quad (21)$$

and Eq. (15) can be rewritten as

$$\begin{aligned} & \int_V {}^1C_{ijrs} {}^1\epsilon_{rs} \delta {}^1\epsilon_{ij} {}^1dv + \int_V {}^1\tau_{ij} \delta {}^1n_{ij} {}^1dv \\ & = {}^2R - \int_V {}^1\tau_{ij} \delta {}^1e_{ij} {}^1dv \end{aligned} \quad (22)$$

which, as Eq. (14), is a nonlinear equation in the incremental displacements  $u_i$ .

### 2.3 Linearization of Equilibrium Equations

It should be noted that Eqs. (14) and (22) are, theoretically, equivalent and provided the appropriate constitutive relations are used, the equations yield identical solutions. However, as will be seen, the finite element matrices established for solution are different.

The solution of Eq. (14) and of Eq. (22), which are equivalent to Eqs. (7) and (15), respectively, cannot be calculated directly, since they are nonlinear in the displacement increments. Approximate solutions can be obtained by assuming that in Eq. (14)  ${}_0\varepsilon_{ij} = {}_0e_{ij}$  and in Eq. (22),  ${}_1\varepsilon_{ij} = {}_1e_{ij}$ . This means that, in addition to using  $\delta {}_0\varepsilon_{ij} = \delta {}_0e_{ij}$  and  $\delta {}_1\varepsilon_{ij} = \delta {}_1e_{ij}$ , respectively, the incremental constitutive relations employed are

$${}_0S_{ij} = {}_0C_{ijrs} {}_0e_{ij} \quad (23)$$

and

$${}_1S_{ij} = {}_1C_{ijrs} {}_1e_{ij} \quad (24)$$

where  ${}_1S_{ij}$  and  ${}_1e_{ij}$  are considered to be approximately equal to an increment in the Cauchy stress  ${}_1\tau_{ij}$  and Almansi strain  ${}_1\varepsilon_{ij}$ , respectively (see Section 3.4).

### 3. FINITE ELEMENT SOLUTION

In the T.L. formulation the approximate equilibrium equation to be solved is

$$\begin{aligned} \int_V {}^0 C_{ijrs} {}^0 e_{rs} \delta {}^0 e_{ij} {}^0 dv + \int_V {}^1 S_{ij} \delta {}^0 n_{ij} {}^0 dv \\ = {}^2 R - \int_V {}^1 S_{ij} \delta {}^0 e_{ij} {}^0 dv \end{aligned} \quad (25)$$

whereas in the U.L. formulation the equation is

$$\begin{aligned} \int_V {}^1 C_{ijrs} {}^1 e_{rs} \delta {}^1 e_{ij} {}^1 dv + \int_V {}^1 \tau_{ij} \delta {}^1 n_{ij} {}^1 dv \\ = {}^2 R - \int_V {}^1 \tau_{ij} \delta {}^1 e_{ij} {}^1 dv \end{aligned} \quad (26)$$

Equations (25) and (26) are linear equations in the incremental displacements and are used as the basis for isoparametric finite element analysis [28] [38]. Referring to the standard procedures for assembling the structure matrices, attention need only be given to the derivation of the matrices corresponding to a single element.

#### 3.1 Finite Element Matrices

In the isoparametric finite element solution the coordinates

and displacements of an element are interpolated using

$${}^i x_j = \sum_k h_k {}^i x_j^k \quad (27)$$

$${}^i u_j = \sum_k h_k {}^i u_j^k \quad (28)$$

where  ${}^i x_j^k$  = coordinate of nodal point k corresponding to direction j and in configuration i,  ${}^i u_j^k$  is defined similarly to  ${}^i x_j^k$  and  $h_k$  = interpolation function associated with nodal point k.

Using Eqs. (27) and (28) to evaluate the displacement derivatives required in the integrals, Eq. (25) becomes, considering a single element

$$\left( {}^1_{0}K_L + {}^1_{0}K_{NL} \right) u = {}^2_R - {}^1_F \quad (29)$$

where  ${}^1_{0}K_L u$ ,  ${}^1_{0}K_{NL} u$  and  ${}^1_F$  are obtained from the finite element

evaluation of  $\int_V {}^0 C_{ijrs} {}^0 e_{rs} \delta {}^0 e_{ij} {}^0 dv$ ,  $\int_V {}^1 S_{ij} \delta {}^0 n_{ij} {}^0 dv$

and  $\int_V {}^1 S_{ij} \delta {}^0 e_{ij} {}^0 dv$ , respectively,

i.e.

$${}^1_{0}K_L = \int_V {}^1_{0}B_L^T {}^0 C {}^1_{0}B_L {}^0 dv \quad (30)$$

$${}^1_{0}K_{NL} = \int_V {}^1_{0}B_{NL}^T {}^1_S {}^1_{0}B_{NL} {}^0 dv \quad (31)$$

$${}^1_0 F = \int_{0^1_V} {}^1_0 B_L^T {}^1_0 \tilde{S} {}^1_0 dv \quad (32)$$

In the equations  ${}^1_0 B_L$  and  ${}^1_0 B_{NL}$  are linear and nonlinear strain displacement transformation matrices,  ${}^1_0 C$  is the material property matrix,  ${}^1_0 S$  is a matrix of 2nd Piola - Kirchhoff stresses, and  ${}^1_0 \tilde{S}$  is a vector of these stresses. All matrix elements correspond to configuration 1 and are defined with respect to configuration 0.

Similarly, the finite element solution of Eq. (26), which was obtained using the U.L. formulation, results into

$$\left( {}^1_1 K_L + {}^1_1 K_{NL} \right) u = {}^2_R - {}^1_1 F \quad (33)$$

where

$${}^1_1 K_L = \int_{1^1_V} {}^1_1 B_L^T {}^1_1 C {}^1_1 B_L {}^1_1 dv \quad (34)$$

$${}^1_1 K_{NL} = \int_{1^1_V} {}^1_1 B_{NL}^T {}^1_1 T {}^1_1 B_{NL} {}^1_1 dv \quad (35)$$

and

$${}^1_1 F = \int_{1^1_V} {}^1_1 B_L^T {}^1_1 \tilde{T} {}^1_1 dv \quad (36)$$

In Eqs. (34) to (36) the elements of the linear and nonlinear strain-displacement transformation matrices  ${}^1_1 B_L$  and  ${}^1_1 B_{NL}$ , respectively, and the elements of the material property matrix  ${}^1_1 C$  correspond to and are

defined with respect to configuration 1,  ${}^1_T$  is a matrix and  ${}^1\tilde{T}$  is a vector of Cauchy stresses in configuration 1. It should be noted that the matrix elements are functions of the natural element coordinates and that the volume integrations are performed using a coordinate change from Cartesian to natural coordinates [38]. As an example, Table 1 shows the strain displacement and stress matrices used for two-dimensional analysis (plane stress and plane strain) in the U.L. and T.L. formulations.

### 3.2 Dynamic Analysis

In dynamic analysis, the applied body forces include inertia forces. Assuming that the mass of the body considered is preserved, the inertia forces are conservative and can in both formulations be evaluated using the initial configuration 0 as reference. Using the standard finite element formulation to evaluate the element mass matrix [38], the incremental equilibrium equation for a single element in the T.L. formulation is

$$\begin{pmatrix} {}^1K_L & + & {}^1K_{NL} \\ 0 & & 0 \end{pmatrix} u = {}^2R - {}^1F - M {}^2\ddot{u} \quad (37)$$

and in the U.L. formulation this equation is

$$\begin{pmatrix} {}^1K_L & + & {}^1K_{NL} \\ 1 & & 1 \end{pmatrix} u = {}^2R - {}^1F - M {}^2\ddot{u} \quad (38)$$

where  ${}^2\ddot{u}$  is a vector of the element nodal point accelerations in configuration 2, and M is the element mass matrix calculated using the original configuration of the body. In Eqs. (37) and (38), damping effects usually defined by a matrix C have been ignored [2].

TABLE 1 MATRICES USED IN TWO-DIMENSIONAL ANALYSIS

A. UPDATED LAGRANGIAN FORMULATION

1. Incremental Strains

$$1^{\epsilon_{11}} = 1^{u_{1,1}} + \frac{1}{2} [(1^{u_{1,1}})^2 + (1^{u_{2,1}})^2]$$

$$1^{\epsilon_{22}} = 1^{u_{2,2}} + \frac{1}{2} [(1^{u_{1,2}})^2 + (1^{u_{2,2}})^2]$$

$$1^{\epsilon_{12}} = \frac{1}{2} [1^{u_{1,2}} + 1^{u_{2,1}}] + \frac{1}{2} [1^{u_{1,1}} 1^{u_{1,2}} + 1^{u_{2,1}} 1^{u_{2,2}}]$$

where  $1^{u_{i,j}} = \frac{\partial u_i}{\partial 1^x_j}$

2. Linear Strain Displacement Transformation Matrix

Using  $1^e = 1^B_L u$

where  $1^e = [1^{\epsilon_{11}} \quad 1^{\epsilon_{22}} \quad 2^{\epsilon_{12}}]^T$ ;  $u^T = [u_1^1 \quad u_2^1 \quad u_1^2 \quad u_2^2 \quad \dots \quad u_1^N \quad u_2^N]$

$$1^B_L = \begin{bmatrix} 1^{h_{1,1}} & 0 & 1^{h_{2,1}} & 0 & 1^{h_{3,1}} & 0 & \dots & 1^{h_{N,1}} & 0 \\ 0 & 1^{h_{1,2}} & 0 & 1^{h_{2,2}} & 0 & 1^{h_{3,2}} & \dots & 0 & 1^{h_{N,2}} \\ 1^{h_{1,2}} & 1^{h_{1,1}} & 1^{h_{2,2}} & 1^{h_{2,1}} & 1^{h_{3,2}} & 1^{h_{3,1}} & \dots & 1^{h_{N,2}} & 1^{h_{N,1}} \end{bmatrix}$$

where  $1^{h_{k,j}} = \frac{\partial h_k}{\partial 1^x_j}$ ;  $u_j^k = 2^k u_j^k - 1^k u_j^k$ ; N = number of nodes

TABLE 1 (cont'd.)

3. Nonlinear Strain Displacement Transformation Matrix

$${}^1B_{NL} = \begin{bmatrix} {}^h_{1,1} & 0 & {}^h_{2,1} & 0 & {}^h_{3,1} & 0 & \dots & {}^h_{N,1} & 0 \\ {}^h_{1,2} & 0 & {}^h_{2,2} & 0 & {}^h_{3,2} & 0 & \dots & {}^h_{N,2} & 0 \\ 0 & {}^h_{1,1} & 0 & {}^h_{2,1} & 0 & {}^h_{3,1} & \dots & 0 & {}^h_{N,1} \\ 0 & {}^h_{1,2} & 0 & {}^h_{2,2} & 0 & {}^h_{3,2} & \dots & 0 & {}^h_{N,2} \end{bmatrix}$$

4. Cauchy Stress Matrix And Stress Vector

$${}^1T = \begin{bmatrix} {}^1\tau_{11} & {}^1\tau_{12} & 0 & 0 \\ {}^1\tau_{21} & {}^1\tau_{22} & 0 & 0 \\ 0 & 0 & {}^1\tau_{11} & {}^1\tau_{12} \\ 0 & 0 & {}^1\tau_{21} & {}^1\tau_{22} \end{bmatrix}; \quad {}^1\tilde{T} = \begin{bmatrix} {}^1\tau_{11} \\ {}^1\tau_{22} \\ {}^1\tau_{12} \end{bmatrix}$$

TABLE 1 (cont'd.)

B. TOTAL LAGRANGIAN FORMULATION

1. Incremental Strains

$$\begin{aligned} \epsilon_{11}^e &= \epsilon_{1,1}^u + \epsilon_{1,1}^u + \epsilon_{1,1}^u + \epsilon_{2,1}^u + \frac{1}{2} [(\epsilon_{1,1}^u)^2 + (\epsilon_{2,1}^u)^2] \\ \epsilon_{22}^e &= \epsilon_{2,2}^u + \epsilon_{1,2}^u + \epsilon_{2,2}^u + \epsilon_{1,2}^u + \frac{1}{2} [(\epsilon_{1,2}^u)^2 + (\epsilon_{2,2}^u)^2] \\ \epsilon_{12}^e &= \frac{1}{2} [\epsilon_{1,2}^u + \epsilon_{2,1}^u] + \frac{1}{2} [\epsilon_{1,1}^u \epsilon_{1,2}^u + \epsilon_{2,1}^u \epsilon_{2,2}^u + \epsilon_{1,2}^u \epsilon_{1,1}^u + \\ &\quad \epsilon_{2,2}^u \epsilon_{2,1}^u] + \frac{1}{2} [\epsilon_{1,1}^u \epsilon_{1,2}^u + \epsilon_{2,1}^u \epsilon_{2,2}^u] \end{aligned}$$

where  $\epsilon_{i,j}^u = \frac{\partial u_i}{\partial x_j}$

2. Linear Strain Displacement Transformation Matrix

Using  $\epsilon^e = \epsilon_L^B u$

where  $\epsilon^T = \begin{bmatrix} \epsilon_{11}^e & \epsilon_{22}^e & 2\epsilon_{12}^e \end{bmatrix}$ ;  $u^T = \begin{bmatrix} u_1^1 & u_2^1 & u_1^2 & u_2^2 & \dots & u_1^N & u_2^N \end{bmatrix}$

$$\epsilon_L^B = \epsilon_{L0}^B + \epsilon_{L1}^B$$

TABLE 1 (cont'd.)

Then

$${}^1_{0}B_{0}L_{0} = \begin{bmatrix} o^{h_{1,1}} & 0 & o^{h_{2,1}} & 0 & o^{h_{3,1}} & 0 & \dots & o^{h_{N,1}} & 0 \\ 0 & o^{h_{1,2}} & 0 & o^{h_{2,2}} & 0 & o^{h_{3,2}} & \dots & 0 & o^{h_{N,2}} \\ o^{h_{1,2}} & o^{h_{1,1}} & o^{h_{2,2}} & o^{h_{2,1}} & o^{h_{3,2}} & o^{h_{3,1}} & \dots & o^{h_{N,2}} & o^{h_{N,1}} \end{bmatrix}$$

where  $o^{h_{k,j}} = \frac{\partial h_k}{\partial x_j}$  ;  $u_j^k = 2u_j^k - 1u_j^k$  ; N = number of nodes

and

$${}^1_{0}B_{0}L_{1} = \begin{bmatrix} \ell_{11} o^{h_{1,1}} & & & & & & & & \ell_{21} o^{h_{2,1}} \\ \ell_{12} o^{h_{1,2}} & & & & & & & & \ell_{22} o^{h_{2,2}} \\ (\ell_{11} o^{h_{1,2}} + \ell_{12} o^{h_{1,1}}) & & & & & & & & (\ell_{21} o^{h_{2,2}} + \ell_{22} o^{h_{2,1}}) \\ \dots & \ell_{11} o^{h_{N,1}} & & & & & & & \ell_{21} o^{h_{N,1}} \\ \dots & \ell_{12} o^{h_{N,2}} & & & & & & & \ell_{22} o^{h_{N,2}} \\ \dots & (\ell_{11} o^{h_{N,2}} + \ell_{12} o^{h_{N,1}}) & & & & & & & (\ell_{21} o^{h_{N,2}} + \ell_{22} o^{h_{N,1}}) \end{bmatrix}$$

TABLE 1 (contd.)

where

$$\ell_{11} = \sum_{k=1}^N h_{o^k,1} u_1^k ; \ell_{22} = \sum_{k=1}^N h_{o^k,2} u_2^k ; \ell_{21} = \sum_{k=1}^N h_{o^k,1} u_2^k ; \ell_{12} = \sum_{k=1}^N h_{o^k,2} u_1^k$$

3. Nonlinear Strain Displacement Transformation Matrix

$${}^1S_{o^{NL}} = \begin{bmatrix} h_{o^1,1} & 0 & h_{o^2,1} & 0 & h_{o^3,1} & 0 & \dots & h_{o^N,1} & 0 \\ h_{o^1,2} & 0 & h_{o^2,2} & 0 & h_{o^3,2} & 0 & \dots & h_{o^N,2} & 0 \\ 0 & h_{o^1,1} & 0 & h_{o^2,1} & 0 & h_{o^3,1} & \dots & 0 & h_{o^N,1} \\ 0 & h_{o^1,2} & 0 & h_{o^2,2} & 0 & h_{o^3,2} & \dots & 0 & h_{o^N,2} \end{bmatrix}$$

4. 2nd Piola-Kirchhoff Stress Matrix and Vector

$${}^1S_o = \begin{bmatrix} {}^1S_{o^{11}} & {}^1S_{o^{12}} & 0 & 0 \\ {}^1S_{o^{21}} & {}^1S_{o^{22}} & 0 & 0 \\ 0 & 0 & {}^1S_{o^{11}} & {}^1S_{o^{12}} \\ 0 & 0 & {}^1S_{o^{21}} & {}^1S_{o^{22}} \end{bmatrix} ;$$

$${}^1\tilde{S}_o = \begin{bmatrix} {}^1S_{o^{11}} \\ {}^1S_{o^{22}} \\ {}^1S_{o^{12}} \end{bmatrix}$$

### 3.3 Equilibrium Iteration

It is important to realize that Eqs. (37) and (38) are only approximations to the actual equations to be solved in each time step, i.e. Eqs. (7) and (15), respectively. Depending on the nonlinearities in the system, the linearization of Eqs. (14) and (22) may introduce errors which ultimately result into solution instability. For this reason it may be necessary to iterate in each load step until, within the necessary assumptions on the variation of the material constants and the numerical time integration, Eqs. (7) and (15) are satisfied to a required tolerance. The equation used in the T.L. formulation is

$$\begin{pmatrix} 1_{oK_L} & + & 1_{oK_{NL}} \end{pmatrix} \Delta u^{(i)} = 2_R - 2_F^{(i)} - M 2_u^{(i)} \quad i = 1, 2, 3, \dots \quad (39)$$

where  $2_u^{(i+1)} = 2_u^{(i)} + \Delta u^{(i)}$ ,  $2_u^{(1)} = 1_u + u$ , and  $2_u^{(i)}$ ,  $2_F^{(i)}$  are accelerations and internal resisting forces obtained using the displacement approximation  $2_u^{(i)}$ . The acceleration approximation  $2_u^{(i)}$  depends on the numerical integration scheme used; and  $2_F^{(i)}$  is the finite element evaluation of  $\int_V 2_{S_{ij}}^{(i)} \delta_{o\epsilon_{ij}}^{(i)} dv$ , where the superscript  $i$  shows that stresses and strains are evaluated using  $2_u^{(i)}$ .

In the U.L. formulation the equation used for equilibrium iteration is

$$\begin{pmatrix} 1_{lK_L} & + & 1_{lK_{NL}} \end{pmatrix} \Delta u^{(i)} = 2_R - 2_F^{(i)} - M 2_u^{(i)} \quad (40)$$

where the  $i$ 'th displacement and acceleration approximations are calculated as above, and  ${}^2_1F^{(i)}$  is the finite element evaluation of

$$\int_{V^{(i)}} {}^2\tau_{ij}^{(i)} \delta {}^2e_{ij}^{(i)} dv^{(i)} = \int_{V^{(i)}} {}^2_1S_{ij}^{(i)} \delta {}^2_1e_{ij}^{(i)} dv.$$

It may be noted that the equilibrium iterations correspond to a modified Newton iteration within each load step [38]. Table 2 summarizes the step-by-step algorithm used in NONSAP. For details on the derivation of the algorithm reference is made to [ 2] [ 3].

### 3.4 Constitutive Relations

Since the T.L. and U.L. formulations are, mathematically, equivalent but the constitutive relations used are defined differently, the choice between the use of either formulation depends to a large degree on the available material definition. If a T.L. constitutive relation is available, then in order to use the U.L. formulation the material tensor must be transformed, and vice versa [22]. In the T.L. formulation the material property tensor  ${}^k_0C_{ijrs}$  relates the 2nd Piola - Kirchhoff stress tensor  ${}^k_0S_{ij}$  to the Green-Lagrange strain tensor  ${}^k_0e_{rs}$  with the reference configuration 0

$${}^k_0S_{ij} = {}^k_0C_{ijrs} {}^k_0e_{rs} \quad (41)$$

where  $k$  is the configuration in which the stresses and strains occur. In the U.L. formulation the equivalent constitutive relation is [ 8],

$${}^k\tau_{ij} = {}^kC_{ijrs} {}^k e_{rs} \quad (42)$$

TABLE 2 SUMMARY OF STEP-BY-STEP INTEGRATION

(For notation used and the derivation of the algorithm, see Reference 2)

INITIAL CALCULATIONS - - -

1. Form linear stiffness matrix  $K$ , mass matrix  $M$  and damping matrix  $C$ ; initialize  $u_0, \dot{u}_0, \ddot{u}_0$

2. Calculate the following constants:

$$\theta \geq 1.37 \quad ; \quad \tau = \theta \Delta t \quad ; \quad tol \leq 0.01 \quad ; \quad nitem \geq 3$$

$$a_0 = 6/\tau^2 \quad a_1 = 3/\tau \quad a_2 = 2a_1 \quad a_3 = \tau/2 \quad a_4 = a_0/\theta$$

$$a_5 = -a_0/\theta \quad a_6 = 1 - 3/\theta \quad a_7 = \Delta t/2 \quad a_8 = \Delta t^2/6$$

3. Form effective linear stiffness matrix:  $\tilde{K} = K + a_0 M + a_1 C$

4. In linear analysis triangularize  $\tilde{K}$

FOR EACH TIMESTEP - - -

A. IN LINEAR ANALYSIS

(i) Form effective loadvector:

$$\tilde{R}_t = R_t + \theta(R_{t+\Delta t} - R_t) + M(a_0 u_t + a_2 \dot{u}_t + 2\ddot{u}_t) + C(a_1 u_t + 2\dot{u}_t + a_3 \ddot{u}_t)$$

(ii) Solve for displacement increments:

$$\tilde{K} \Delta u_t = \tilde{R}_t \quad ; \quad \Delta u_t = u_{t+\tau} - u_t$$

(iii) Go to C.

B. IN NONLINEAR ANALYSIS

(i) Update  $\tilde{K}$  for nonlinear stiffness effects to obtain  $\tilde{K}_t$  and triangularize

(ii) Form effective loadvector

$$\tilde{R}_t = R_t + \theta(R_{t+\Delta t} - R_t) + M(a_2 \dot{u}_t + 2\ddot{u}_t) + C(2\dot{u}_t + a_3 \ddot{u}_t) - F_t'$$

(iii) Solve for displacement increments:

$$\tilde{K}_t \Delta u_t = \tilde{R}_t$$

(iv) If required, iterate for dynamic equilibrium; then initialize  $\Delta u_t^{(1)} = \Delta u_t, i = 0$

(a)  $i = i + 1$

(b) Calculate  $i$ 'th approximation to accelerations, velocities, and displacements:

$$\ddot{u}_{t+\tau}^{(i)} = a_0 \Delta u_t^{(i)} - a_2 \dot{u}_t - 2\ddot{u}_t \quad ; \quad \dot{u}_{t+\tau}^{(i)} = a_1 \Delta u_t^{(i)} - 2\dot{u}_t - a_3 \ddot{u}_t$$

$$u_{t+\tau}^{(i)} = u_t + \Delta u_t^{(i)}$$

(c) Calculate  $i$ 'th out-of-balance loads:  $R_{t+\tau}^{(i)} = R_t + \theta(R_{t+\Delta t} - R_t) - M\ddot{u}_{t+\tau}^{(i)} - C\dot{u}_{t+\tau}^{(i)} - F_{t+\tau}^{(i)}$

(d) Solve for  $i$ 'th correction to displacement increments:  $\tilde{K}_t \Delta \Delta u_t^{(i)} = R_{t+\tau}^{(i)}$

(e) Calculate new displacement increments:  $\Delta u_t^{(i+1)} = \Delta u_t^{(i)} + \Delta \Delta u_t^{(i)}$

(f) Iteration convergence if  $\|\Delta \Delta u_t^{(i)}\|_2 / \|\Delta u_t^{(i+1)} + u_t\|_2 < tol$

If convergence:  $\Delta u_t = \Delta u_t^{(i+1)}$  and go to C;

If no convergence and  $i < nitem$ :

go to (a); otherwise restart using a smaller time step size.

C. CALCULATE NEW ACCELERATIONS, VELOCITIES, AND DISPLACEMENTS

$$\ddot{u}_{t+\Delta t} = a_4 \Delta u_t + a_5 \dot{u}_t + a_6 \ddot{u}_t \quad ; \quad \dot{u}_{t+\Delta t} = \dot{u}_t + a_7 (\ddot{u}_{t+\Delta t} + \ddot{u}_t) \quad ;$$

$$u_{t+\Delta t} = u_t + \Delta t \dot{u}_t + a_8 (\ddot{u}_{t+\Delta t} + 2\ddot{u}_t)$$

where  ${}^k\tau_{ij}$  and  ${}^k\epsilon_{rs}$  are Cauchy stress and Almansi strain tensors in configuration  $k$ , respectively, ( ${}^k\tau_{ij} \equiv k\tau_{ij}$ ,  ${}^k\epsilon_{rs} \equiv k\epsilon_{rs}$ ) and

$${}^k_C o_{mnpq} = \frac{o_\rho}{k_\rho} \quad o^{x_{m,i}} \quad o^{x_{n,j}} \quad k^C_{ijrs} \quad o^{x_{p,r}} \quad o^{x_{q,s}} \quad (43)$$

$${}^k_C k_{mnpq} = \frac{k_\rho}{o_\rho} \quad o^{x_{m,i}} \quad o^{x_{n,j}} \quad o^C_{ijrs} \quad o^{x_{p,r}} \quad o^{x_{q,s}} \quad (44)$$

The incremental relations in Eqs. (13) and (21), and therefore the constitutive approximations in Eqs. (23) and (24) need be derived from Eqs. (41) and (42), respectively. The derivation will depend on if the material is elastic, hyperelastic or hypoelastic [ 8].

In the case of elasticity and hyperelasticity, the incremental constitutive relations Eqs. (23) and (24) are obtained from the instantaneous derivatives of the total stress-strain relations in configuration 1, i.e.  $k = 1$  in Eqs. (41) and (42), respectively. It should be noted that the derivative of the T.L. stress-strain relation in Eq. (41) yields Eq. (13) whereas the derivative of the U.L. stress-strain relation in Eq. (42) relates Cauchy stress increments to Almansi strain increments, and therefore the exact incremental U.L. stress strain relation in Eq. (21) is not obtained. However, with the necessary assumptions pointed out in Section 2.3 the required incremental constitutive relation is obtained in either case. It is important to note that to evaluate the current stresses, in elasticity and hyperelasticity, the total stress-strain relations, Eqs. (41) and (42), are used.

Considering hypoelastic materials, e.g. plasticity using the flow theory, the incremental stress-strain relations only are given

and total stresses must be calculated by adding increments in stresses [ 8] [34].

Because the transformations in Eqs.(43) and (44) would be required, it may be of advantage to use the formulation in which the constitutive relations are given. In case of elasticity, either  ${}^k C_{ijrs}$  or  ${}^k C_{ijrs}$  may be given and in hyperelasticity the T.L. constitutive relation is commonly used [16] [28]. The question of which formulation to use in large strain plastic analysis has not been resolved [12] [13] [19] and is further being investigated.

#### 4. NONCONSERVATIVE LOADING

So far it has been assumed that the loads are independent of the configuration of the body. In practice, therefore, the external loads for each step can be calculated and stored on back-up storage before the actual time integration is carried out. However, when the structure undergoes large displacements or large strains it may be necessary to consider the externally applied loads to be configuration dependent.

An important type of loading, which may need to be considered as nonconservative, is pressure loading [28]. In this case the loading to be used in the T.L. formulation is

$${}^2_t_k \circ da = - \frac{{}^0_p}{2} {}^2_p \circ x_{i,k} \circ n_i \circ da \quad (45)$$

and in the U.L. formulation

$${}^1_t_k \circ da = - \frac{{}^1_p}{2} {}^2_p \circ x_{i,k} \circ n_i \circ da \quad (46)$$

where  ${}^j_n_i$  = component  $i$  of the normal  $n$  in configuration  $j$ , and  ${}^2_p$  = surface pressure in configuration 2. Equation (45) can be written in the form

$$\begin{aligned} {}^2_t_k \circ da &= - \frac{{}^0_p}{2} {}^2_p \circ x_{i,k} \circ n_i \circ da \\ &+ \frac{{}^0_p}{2} {}^2_p \circ x_{i,j} \circ u_{j,k} \circ n_i \circ da \end{aligned} \quad (47)$$

and similarly Eq. (46) becomes

$${}^2_1 t_k \quad {}^1_{da} = - \frac{1}{2} \frac{\rho}{\rho} \quad {}^2_p \quad {}^1_{n_k} \quad {}^1_{da} + \frac{1}{2} \frac{\rho}{\rho} \quad {}^2_p \quad {}^2_{u_{i,k}} \quad {}^1_{n_i} \quad {}^1_{da} \quad (48)$$

where in both formulations the first integral enters the load vector and, assuming that  ${}^2_{u_{i,k}} \approx {}^1_{u_{i,k}}$ , the second integral contributes to the system tangent stiffness matrix. It should be noted that this is a nonsymmetric contribution to the stiffness matrix, and is therefore in practice computationally inefficient to handle. Since equilibrium iterations are probably required in any case, it appears more efficient, at least when pressures are reasonably small, to neglect the contribution of the pressure load to the stiffness matrix. In the iteration the loads are then evaluated as

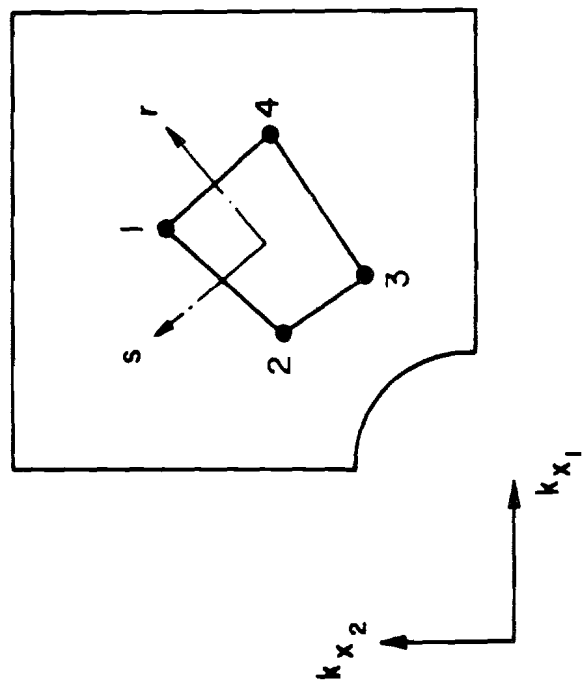
$$- \frac{\rho}{2} \frac{1}{\rho(j)} \quad {}^2_p \quad \frac{\partial^0 x_i}{\partial^2 x_k(j)} \quad {}^0_{n_i} \quad {}^0_{da} \quad \text{and} \quad - \quad {}^2_p \quad {}^2_{n_k(j)} \quad {}^2_{da(j)}$$

in the T.L. and U.L. formulations, respectively, where the right superscript (j) indicates the configuration of the iteration. It is seen that although the same approximations are involved in both formulations, the U.L. formulation requires less numerical operations and seems more natural to use.

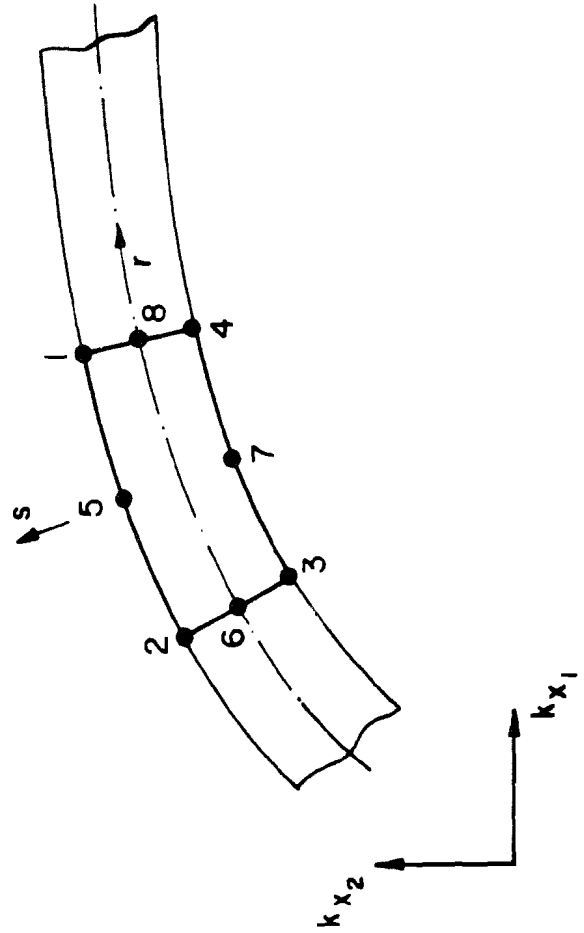
## 5. SAMPLE SOLUTIONS

The analyses presented in the following have been performed using 4-node or 8-node isoparametric two-dimensional elements. The order of Gauss integration has been 2 for the 4-node and 3 for the 8-node elements, respectively. Figure 2 shows a typical 4-node and 8-node element.

The solution algorithm used in NONSAP is summarized in Table 2, where the specific parameters used were  $\theta = 1.4$ ,  $\text{tol} = 0.001$ ,  $\text{nitem} = 20$ .



4-NODE ELEMENT FOR RUBBER SHEET



8-NODE ELEMENT FOR CANTILEVER, ARCHES AND SHELLS

FIGURE 2 ISOPARAMETRIC ELEMENTS USED IN THE SAMPLE SOLUTIONS

## 1. Large Displacement Static Analysis of a Cantilever

The cantilever in Fig. 3 under uniformly distributed load was analyzed using the T.L. and U.L. formulations. The cantilever was idealized using five 8-node plane stress elements.

A solution was obtained for the loading retaining its vertical direction, i.e. conservative loading, and with the loading remaining perpendicular to the top and bottom surfaces of the cantilever, i.e. nonconservative follower loading. In the finite element solution the nonconservative loading is defined by specifying the direction of the nodal loads to pass through two nodal points, the coordinates of which are updated in each load step. In this specific analysis, the top and bottom surface nodal points of the cantilever have been used to define the direction of the loading. The deflection load curves are presented in Fig. 4. The solution obtained from NONSAP for the conservative loading condition is compared with an analytical solution provided by Holden [14]. Excellent agreement has been obtained.

This example was also used to study the influence of the step size when no equilibrium iterations are performed. Figure 5 shows the displacements obtained for different numbers of load steps without equilibrium iteration (see Table 2).

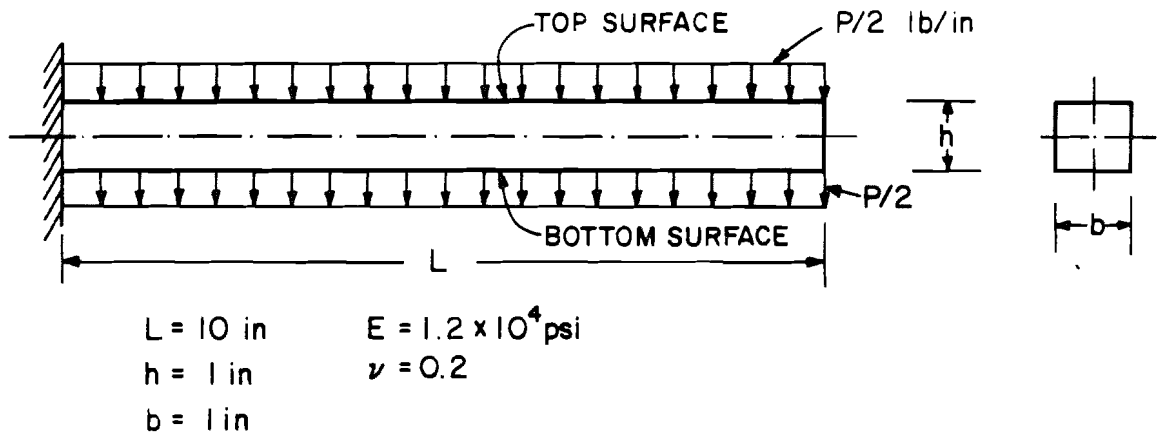


FIGURE 3 CANTILEVER UNDER UNIFORMLY DISTRIBUTED LOAD

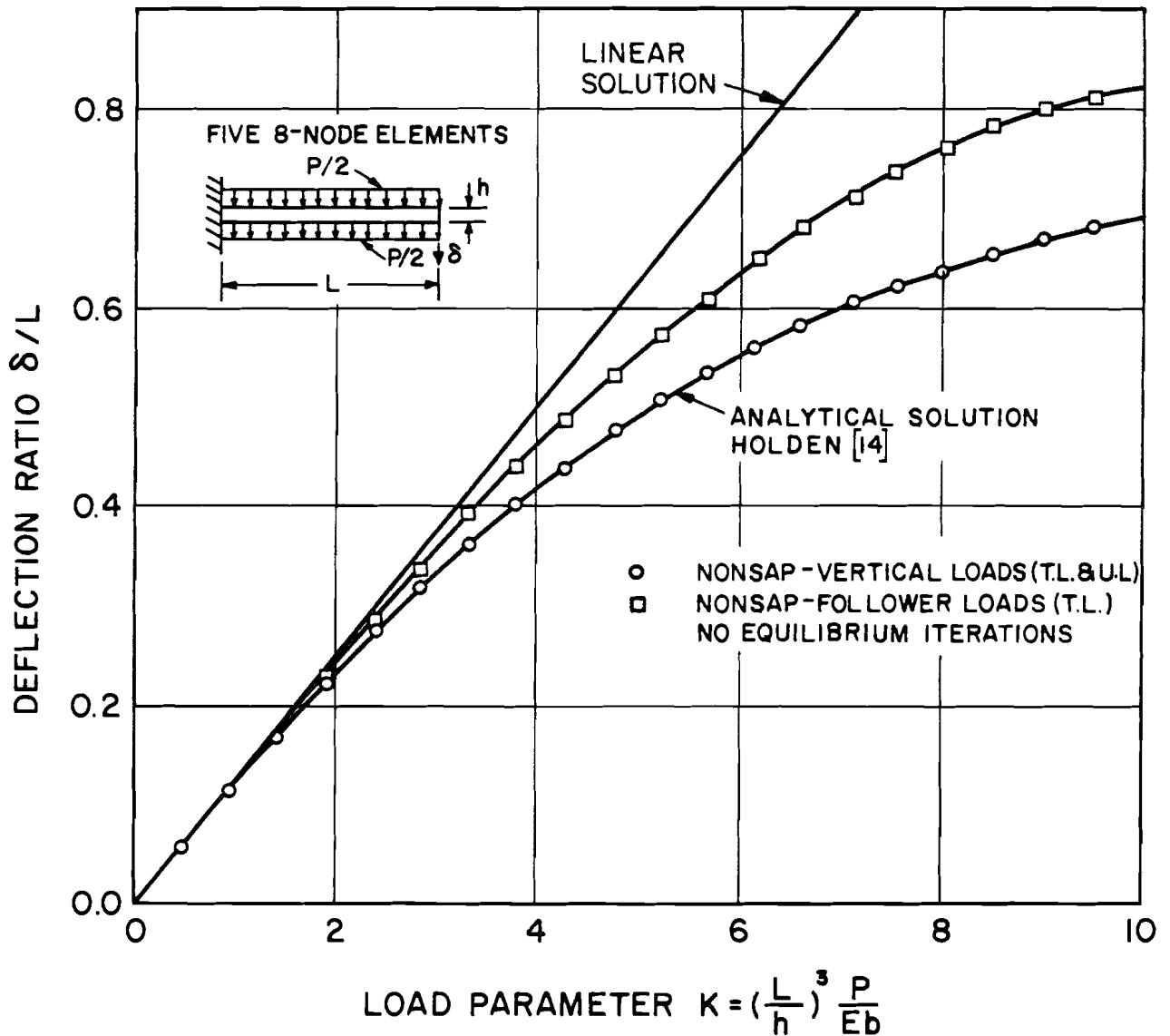


FIGURE 4 LARGE DEFLECTION ANALYSIS OF CANTILEVER UNDER UNIFORMLY DISTRIBUTED LOAD

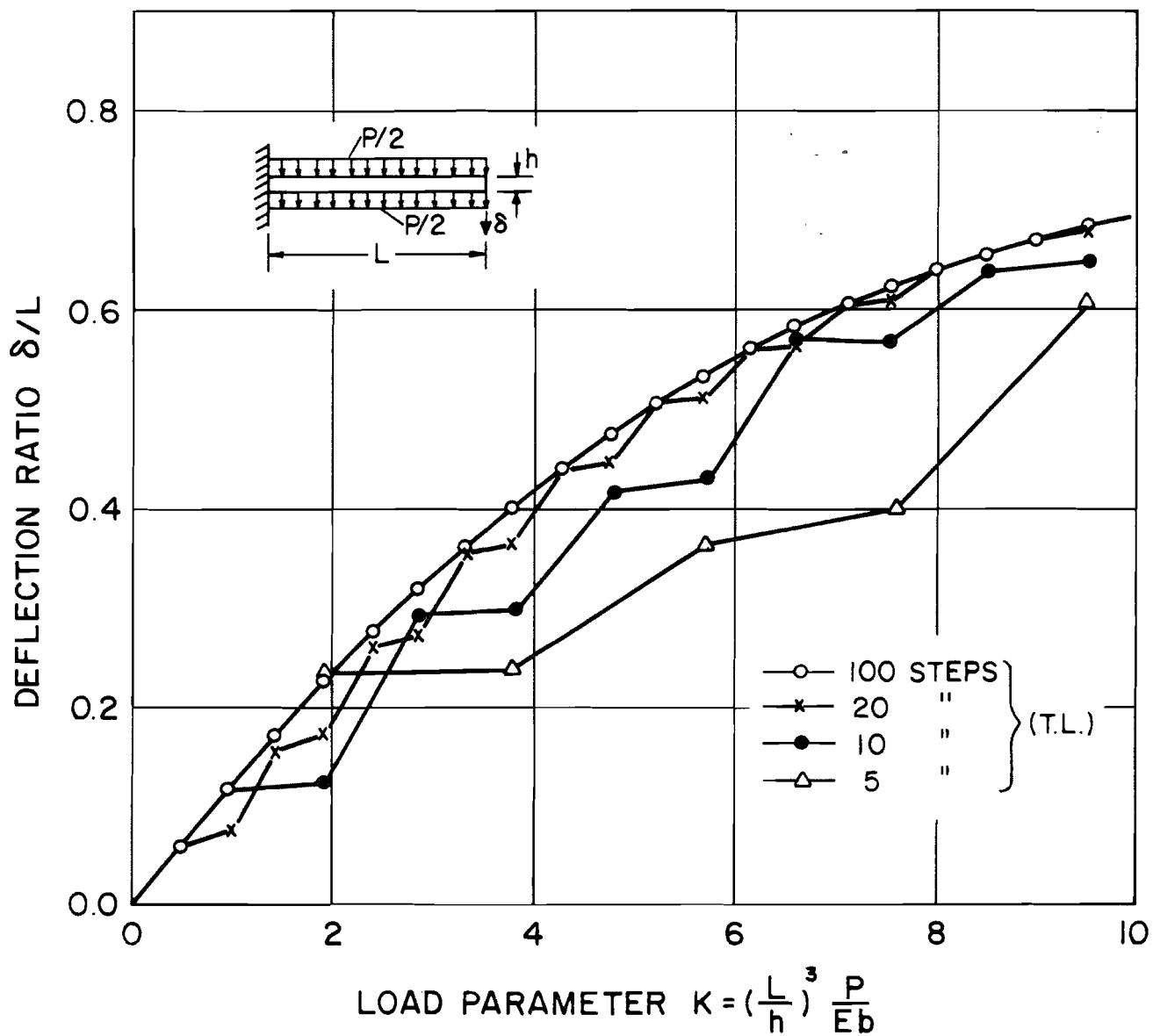
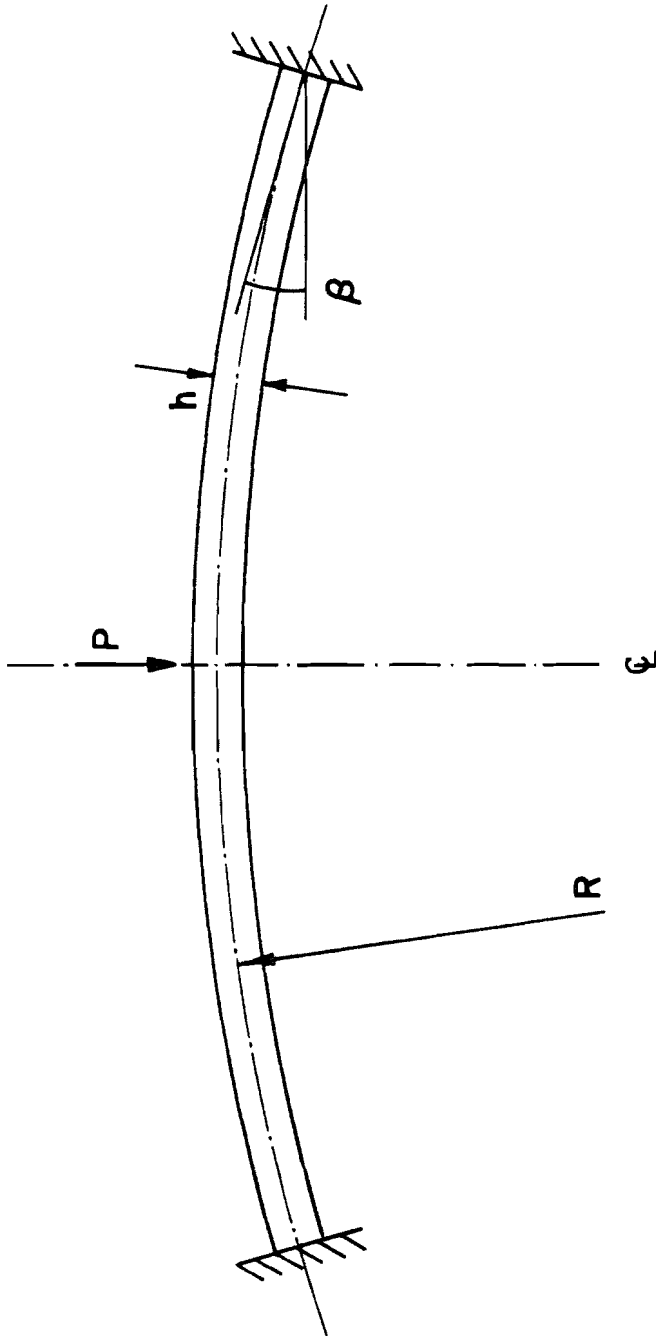


FIGURE 5 LARGE DEFLECTION ANALYSIS OF CANTILEVER  
 INFLUENCE OF STEP SIZE (NO EQUILIBRIUM  
 ITERATIONS)

## 2. Large Displacement Static Analysis of a Shallow Arch

The shallow circular arch shown in Fig. 6 was analyzed for buckling due to a concentrated load at the midpoint of the arch. Six 8-node plane stress elements were used to idealize one half of the arch with symmetric boundary conditions at the arch crown. The arch was analyzed using the T.L. and U.L. formulations, with equilibrium iterations. Figure 7 shows the crown displacement of the arch as calculated by NONSAP. An analytical solution obtained by Schreyer and Masur is also shown [29].

The small difference in results between the T.L. and the U.L. formulations is due to using the same Young's modulus and Poisson ratio in both analyses. Figure 7 shows that the results of the analyses using NONSAP are close to the solution of Schreyer and Masur.



$E = 10 \times 10^6 \text{ psi}$   
 $\nu = 0.25$

LOAD PARAMETER:  
 $\bar{P} = \frac{12\beta R^2}{\pi^2 E h^3} P$

$R = 100 \text{ in}$   
 $h = 2 \text{ in}$   
 $t = 1 \text{ in (WIDTH)}$   
 $\beta = 0.245 \text{ rad}$   
 $\lambda = \beta^2 \frac{R}{h} = 3.0$

FIGURE 6 SHALLOW CIRCULAR ARCH UNDER CONCENTRATED LOAD

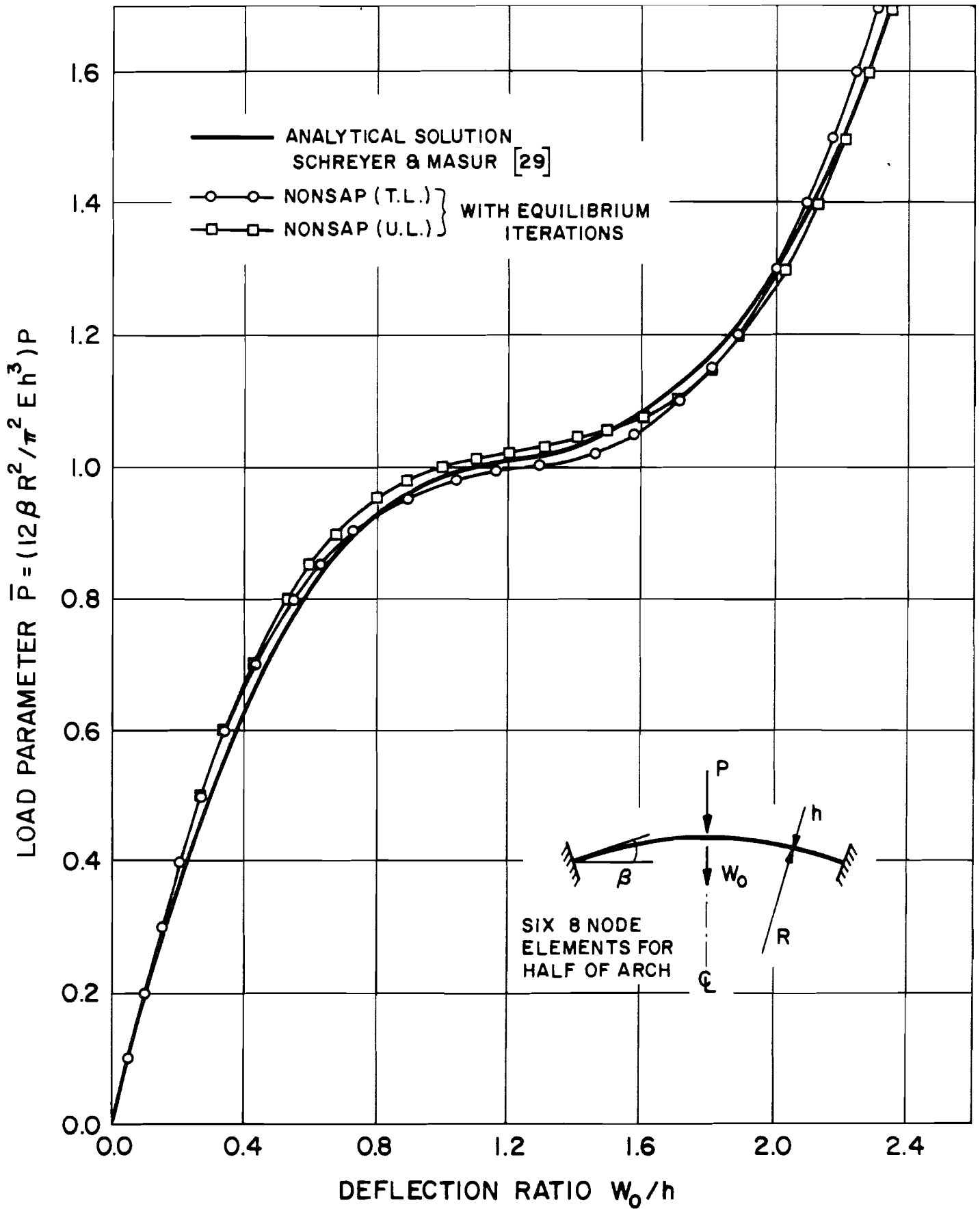
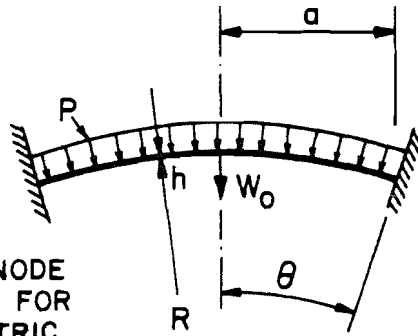


FIGURE 7 LOAD-DEFLECTION CURVE OF A SHALLOW CIRCULAR ARCH

### 3. Large Displacement Static Analysis of a Spherical Shell

A clamped shallow spherical shell subjected to pressure load was analyzed using the T.L. and the U.L. formulations, Fig. 8. Axisymmetric analyses using eight 8-node elements have been performed. The load deflection curve predicted by NONSAP using the T.L. formulation is shown in Fig. 8. The results are compared with an analytical solution of Kornishin and Isanbaeva [18], and a finite element solution of Yeh [37]. Since equilibrium iterations were performed in NONSAP, the oscillating behavior at the beginning of the post-buckling range in Yeh's solution was not obtained.

The U.L. formulation gave almost indistinguishable results to those of the T.L. formulation.



$R = 100$  in  
 $h = 0.5$  in  
 $\theta = 7.1^\circ$   
 $E = 3 \times 10^4$  ksi  
 $\nu = 0.3$

EIGHT 8-NODE  
ELEMENTS FOR  
AXISYMMETRIC  
ANALYSIS

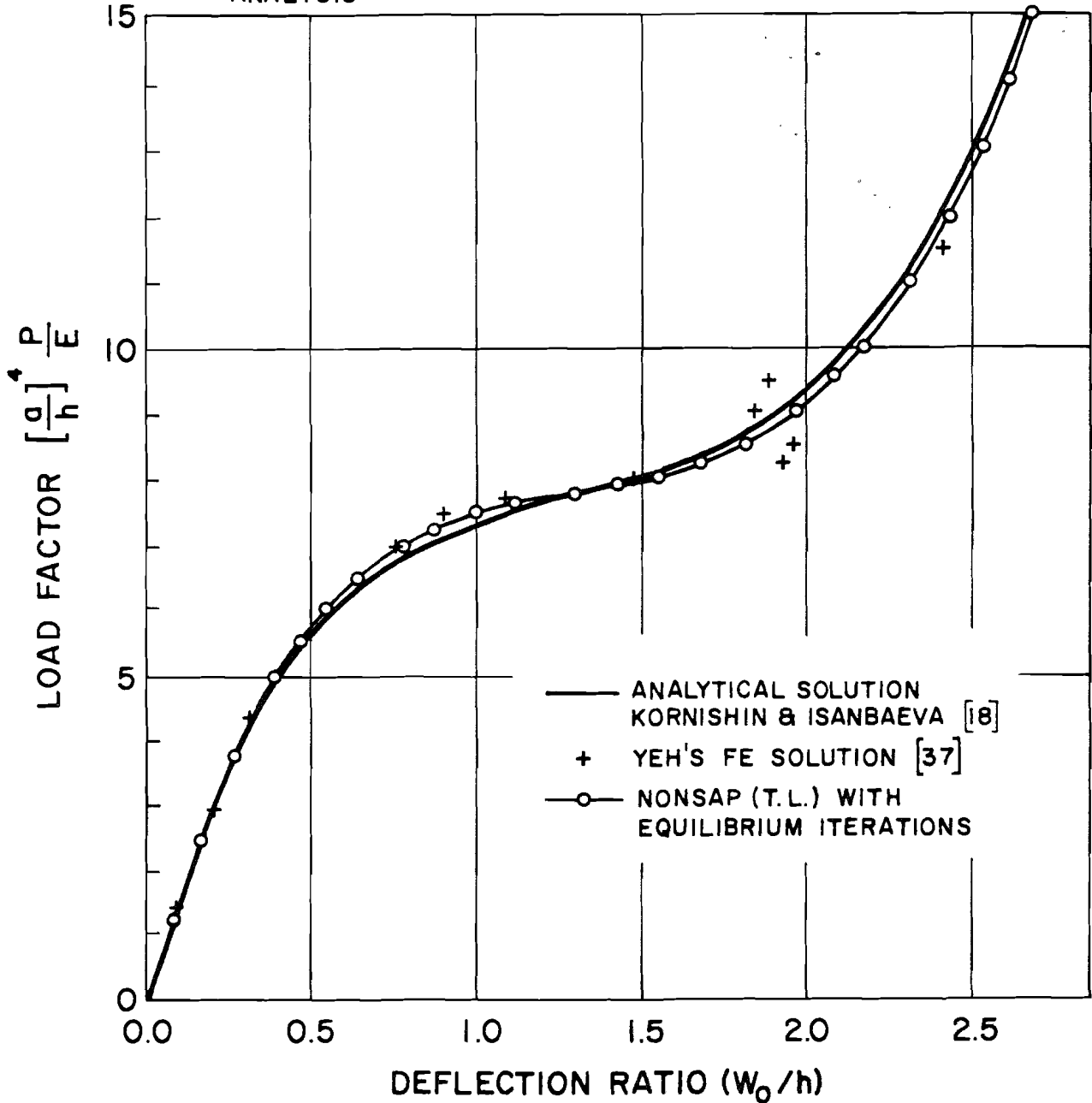


FIGURE 8 LOAD-DEFLECTION CURVE FOR A SHALLOW SPHERICAL SHELL

#### 4. Large Strain and Large Displacement Static and Dynamic Analysis of Rubber Sheet with Hole.

The rubber sheet shown in Fig. 9 was analyzed assuming a Mooney-Rivlin type material for which the incremental stress-strain relations are derived in Appendix A. The specific material constants used for the hyperelastic incompressible material are  $C_1 = 25$  psi,  $C_2 = 7$  psi. These constants are based on an analytical and experimental investigation of the rubber sheet by Iding [16]. The finite element mesh used in the plane stress analysis is shown in Fig. 10. Thirty 4-node elements have been employed. In the static analysis 3 (and 9) equal-sized load increments have been used to reach the final load position, Fig. 11. At this stage, Green-Lagrange strains up to more than 4.5 are measured. Fig. 12 shows the load deflection relations of some characteristic points. These results are in excellent agreement with those of Iding. The results of Iding have been obtained with the computer program developed in Ref [16], but are not given in the reference.

A dynamic analysis was performed for the step load shown in Fig. 13. The selected time step  $\Delta t$  was 0.0015 sec, which is approximately 1/120 of the fundamental period of the sheet. No physical damping was considered. The variation of some displacements as a function of time are shown in Fig. 13 and compared with the corresponding static load deflections.

In all analyses equilibrium iterations have been performed.

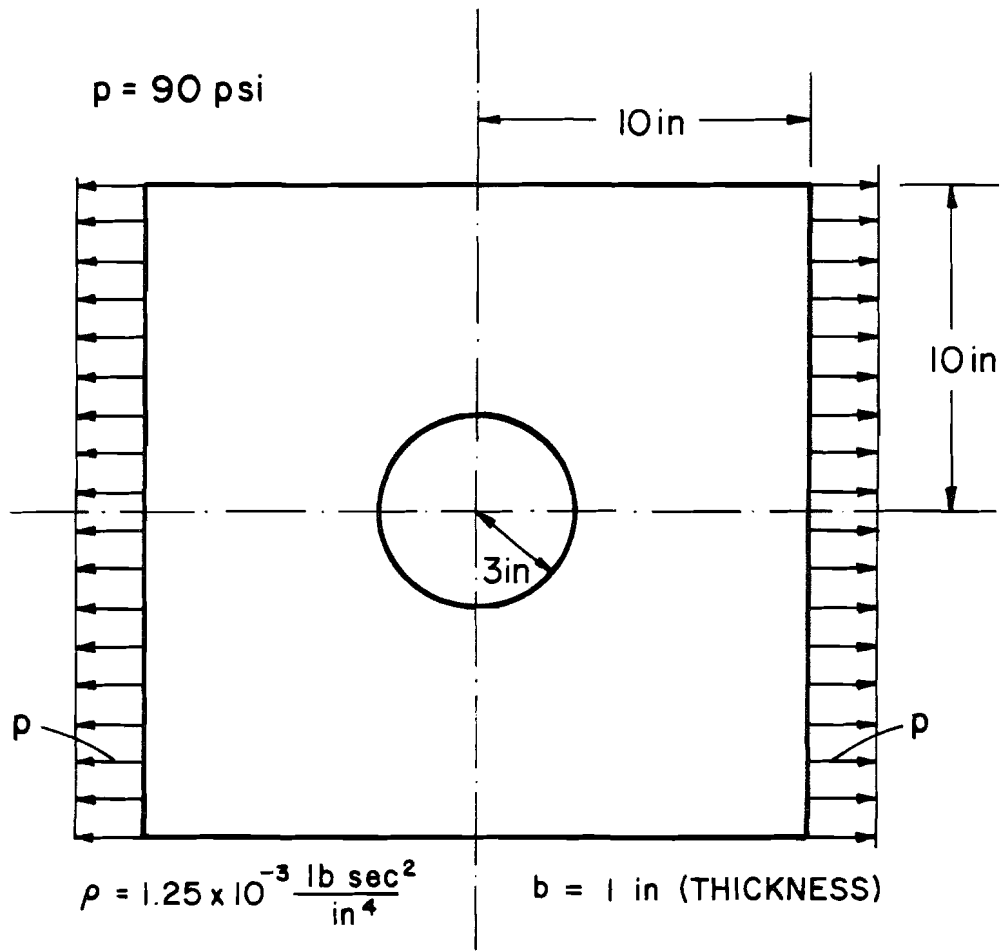


FIGURE 9 RUBBER SHEET WITH HOLE

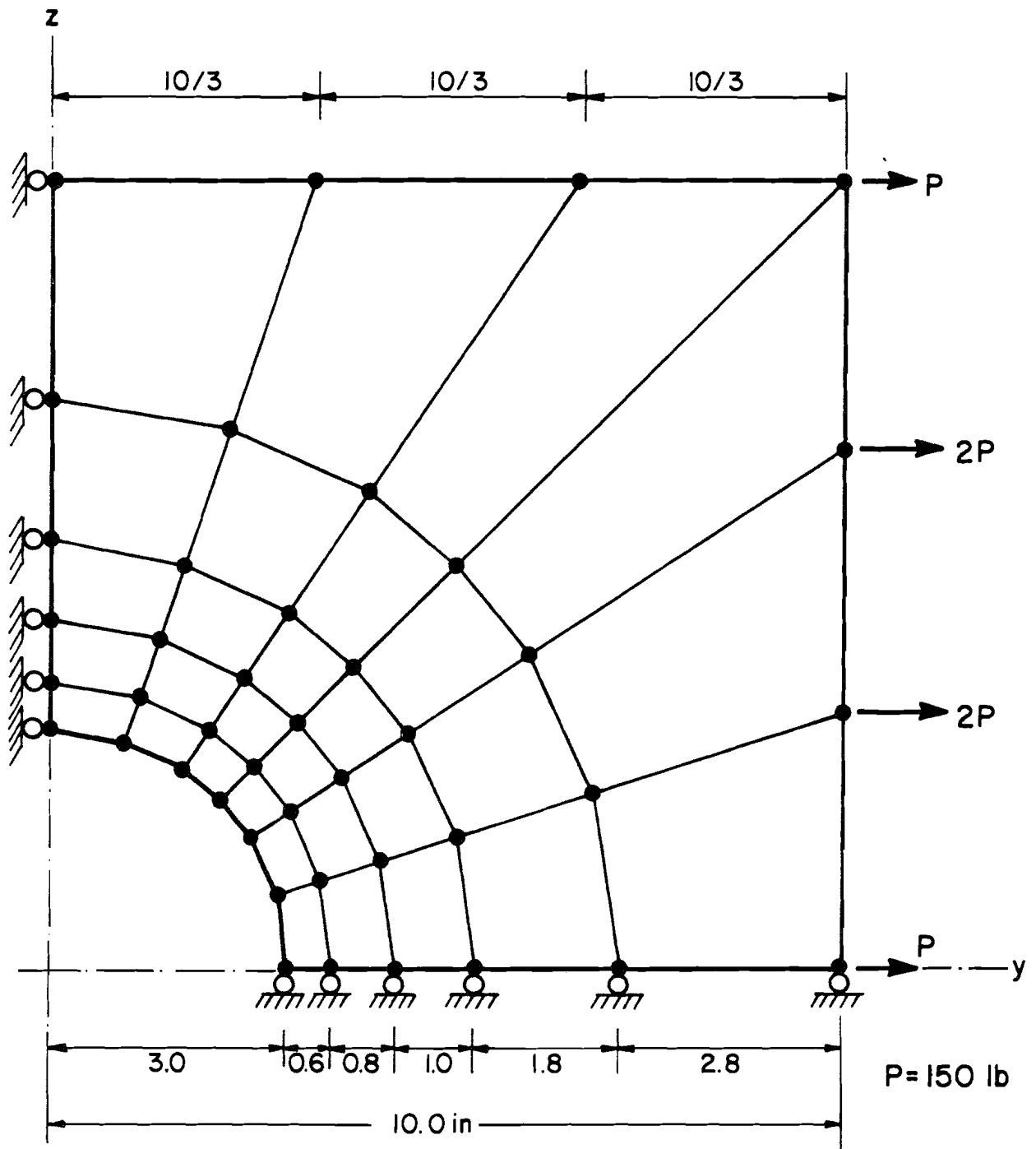


FIGURE 10 FINITE ELEMENT MESH OF RUBBER SHEET

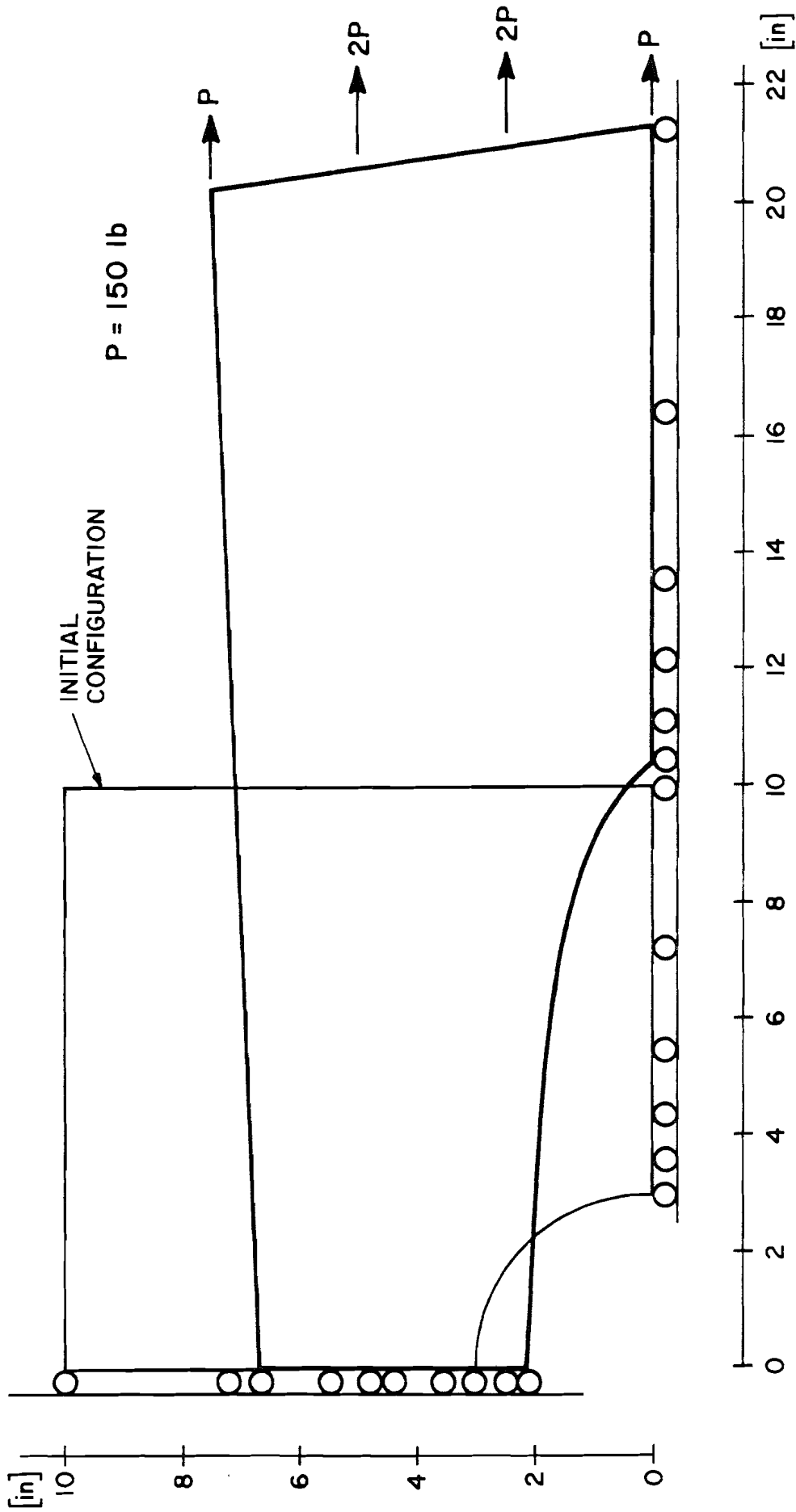


FIGURE II DEFORMED CONFIGURATION DRAWN TO SCALE OF RUBBER SHEET WITH HOLE (STATIC ANALYSIS)

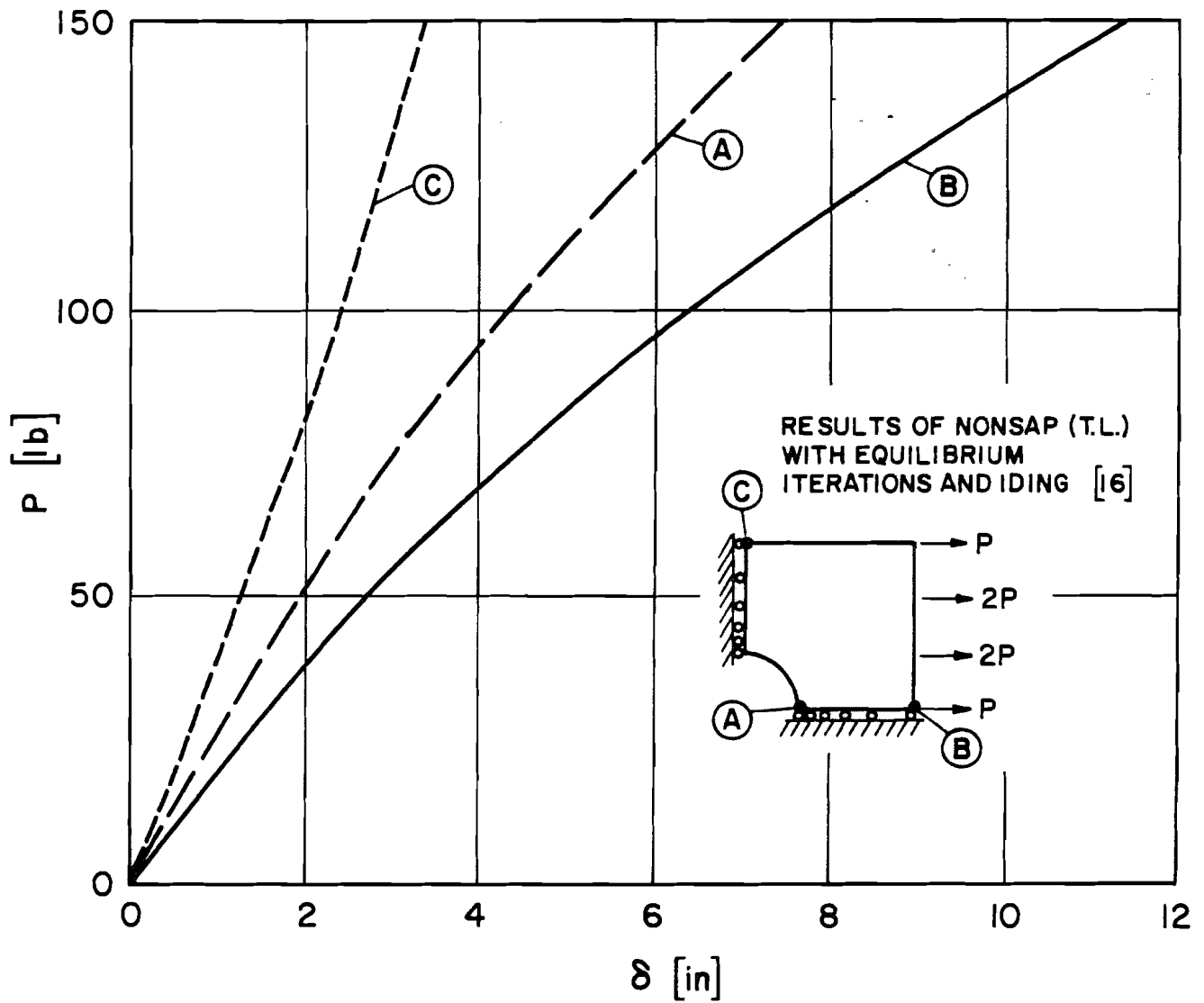


FIGURE 12 LOAD-DEFLECTION CURVE FOR A RUBBER SHEET WITH HOLE (STATIC ANALYSIS)

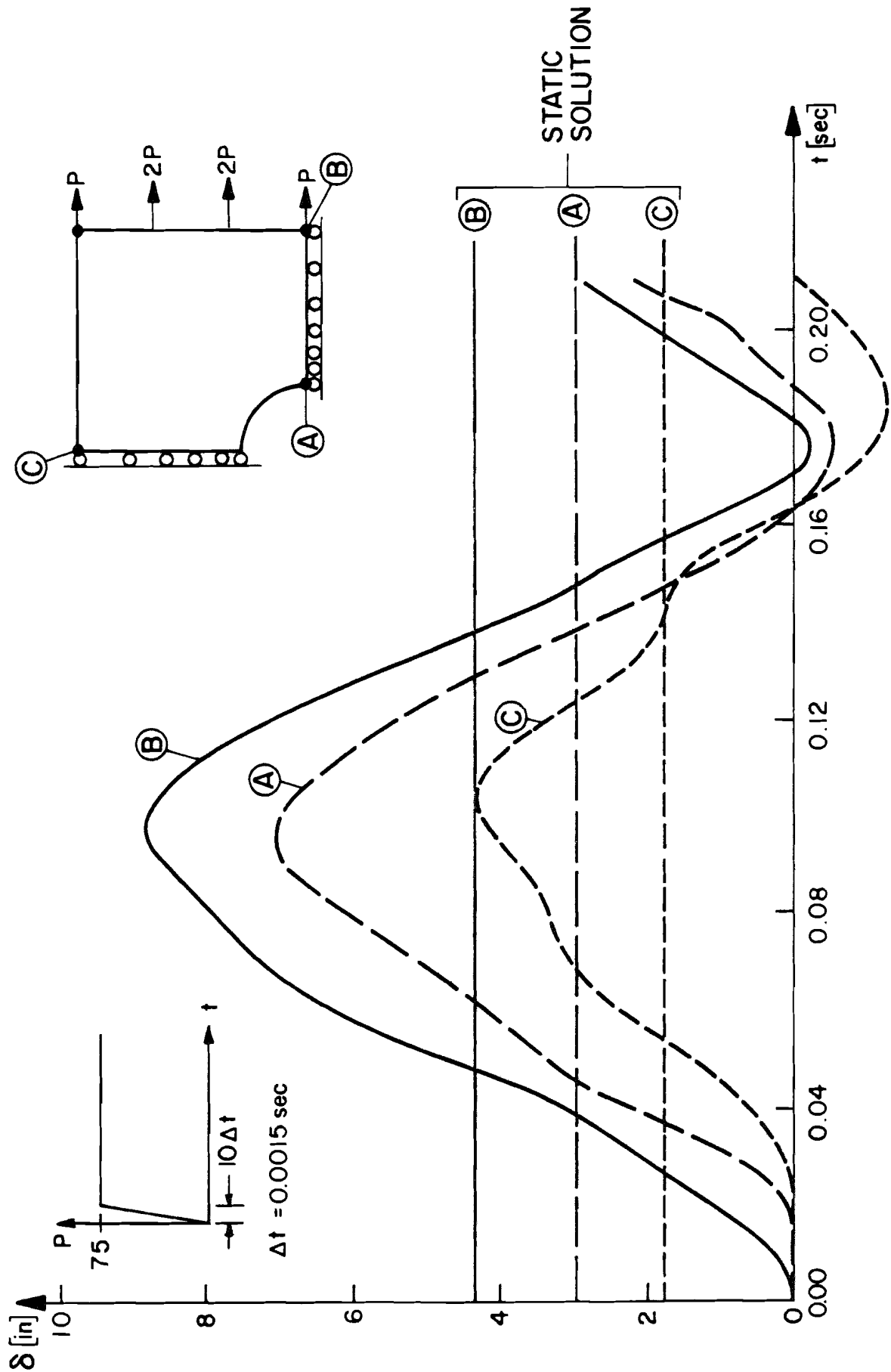
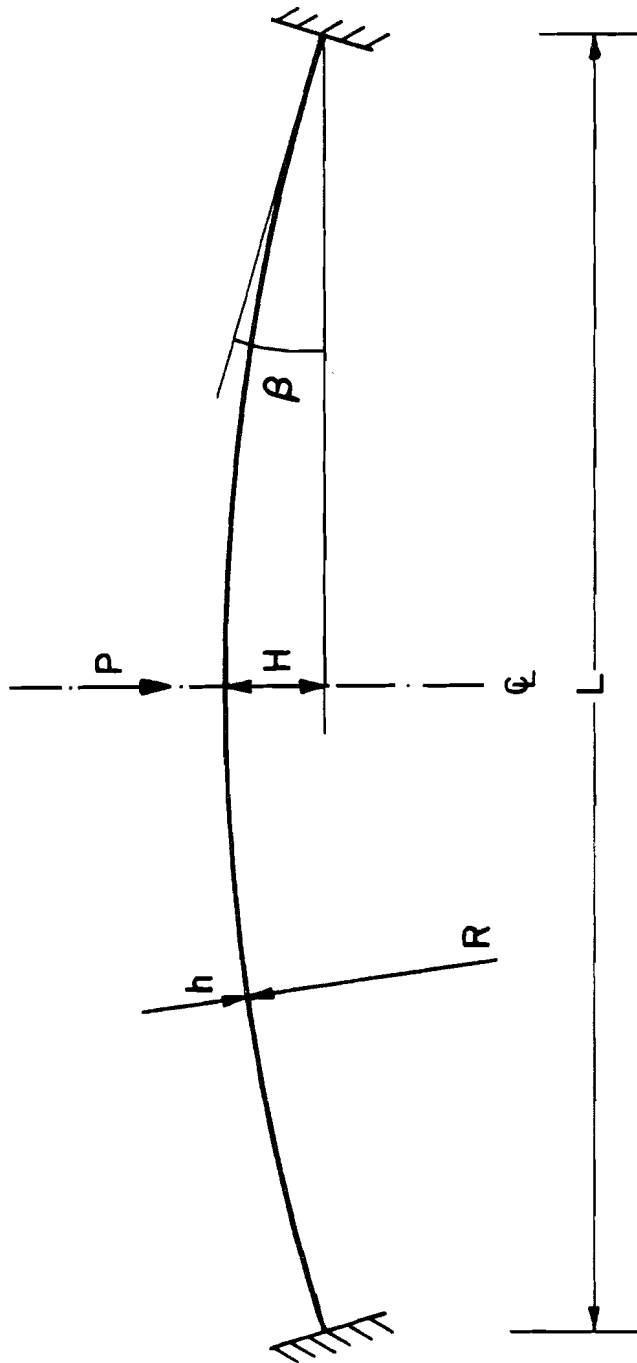


FIGURE 13 DISPLACEMENTS VS. TIME FOR RUBBER SHEET WITH HOLE  
 NONSAP (T.L.) WITH EQUILIBRIUM ITERATIONS

## 5. Large Displacement Static Analysis of a Second Shallow Arch

The clamped circular arch shown in Fig. 14 was analyzed for buckling due to a single static load using the T.L. and U.L. formulations with equilibrium iterations. Considering the symmetry of the structure and loading, half of the arch was idealized by twelve 8-node plane stress elements. Figure 15 shows the calculated load-deflection curve of the arch. The differences in the displacements calculated using the U.L. and T.L. formulations were less than 2 percent.

The same arch was also analyzed by Mallet et al. who used four "equilibrium - based" elements [21]. Dupuis et al. analyzed the arch with curved beam elements, and used this example to demonstrate the convergence of their Lagrangian and 'updated' formulations [5]. In the latter formulation only the nodal points were updated, but not the geometry within the elements. As shown in Fig. 15, the results are very sensitive to the number of elements used and are not satisfactory. Dupuis et al. also compared the calculated results with experimental results by Gjelsvik and Bodner [9], whose predicted buckling load is about ten percent lower than calculated by Mallet. However, it need be realized that an arch with a parameter  $\lambda = 11.6$  is already influenced by antisymmetric buckling modes, which, although possible in the experiment, have not been taken account of in the analyses. The results obtained using NONSAP are therefore satisfactory.



$R = 133.114 \text{ in}$   
 $h = 3/16 \text{ in}$   
 $b = 1.0 \text{ in (WIDTH)}$   
 $L = 34.0 \text{ in}$   
 $H = 1.09 \text{ in}$   
 $\beta = 7.3397^\circ$

$A = 0.188 \text{ in}^2$   
 $I = 0.00055 \text{ in}^4$   
 $E = 10 \times 10^6 \text{ psi}$   
 $\nu = 0.2$   
 $\lambda = \beta^2 \frac{R}{h} = 11.62$

FIGURE 14 SHALLOW CIRCULAR ARCH UNDER CONCENTRATED LOAD

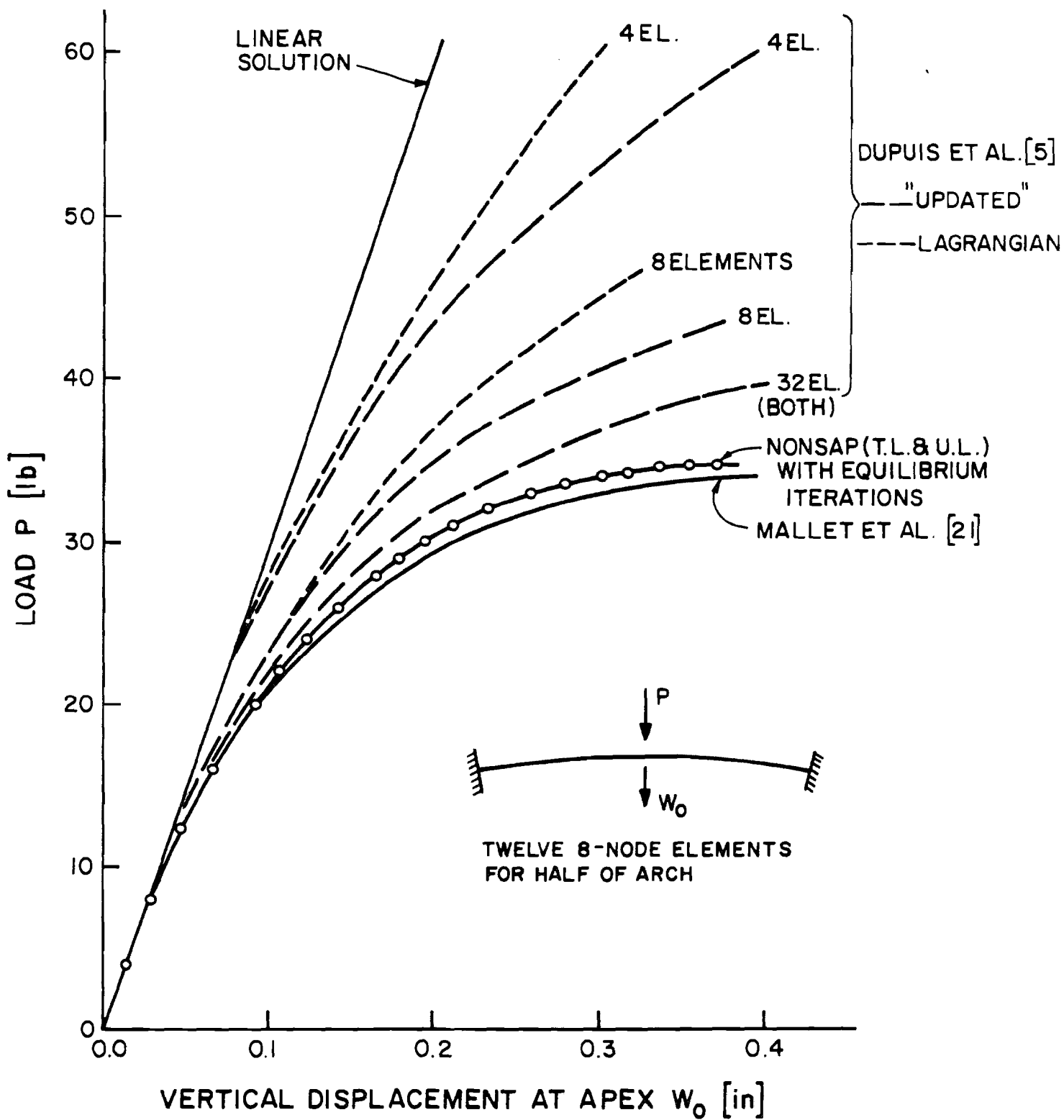


FIGURE 15 LOAD-DEFLECTION CURVE FOR A SHALLOW ARCH UNDER CONCENTRATED LOAD

## 6. Dynamic Snap Buckling of a Shallow Arch

A dynamic buckling analysis of the circular arch shown in Fig. 16 was carried out using six 8-node plane stress elements to idealize half of the symmetric structure. In the analysis the T.L. formulation was used. The uniformly distributed pressure load was applied as a step load. The timestep  $\Delta t$  was selected equal to  $3.315 \times 10^{-5}$  sec, which is approximately 1/70th of the fundamental period of the structure. No physical damping was considered.

The arch is an example of Humphreys' analytical and experimental investigation, who solved the governing differential equation using an analog computer [15]. Humphreys concluded that the buckling load of this arch is not influenced by antisymmetric modes.

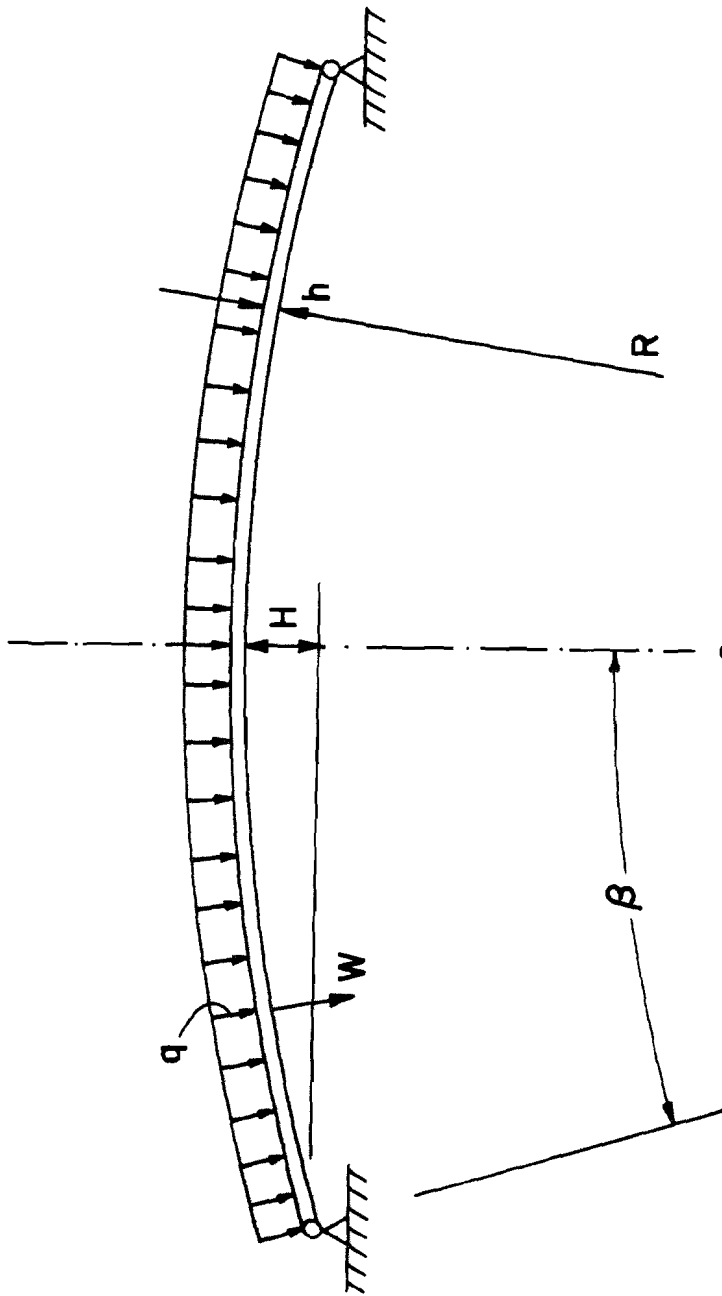
Figure 17 shows the displacement response calculated using NONSAP and obtained by Humphreys. In the figure, the deflection ratio  $\Delta$  defined as

$$\Delta = \frac{\text{average normal deflection } w}{\text{average rise of arch} = H/2}$$

is used. The dynamic buckling of the arch occurs at that load level at which a sudden increase in the deflection ratio  $\Delta$  is measured. Figure 17 shows that at  $p_0 = 0.190$  the arch oscillates about a position of approximately  $\Delta = 0.25$ , and that at  $p_0 = 0.200$  the arch first snaps through, and then oscillates about a position of approximately  $\Delta = 2.5$ . Therefore, the buckling load predicted using NONSAP lies between  $p_0 = 0.190$  and  $p_0 = 0.200$ , which is about 5% lower than predicted by Humphreys.

It should be noted that for a load larger than the buckling load, i.e. for  $p_0 = 0.25$ , the maximum response increases only little. The results using NONSAP for  $p_0 = 0.250$  are in essential agreement with Humphreys' results, where the slightly larger response agrees with the observation that NONSAP predicted a smaller buckling load. The discrepancies in the results can arise from approximations in either analysis. Humphreys' series solution is based on the assumption of shallowness, i.e.  $q$  and  $w$  are measured vertically, and in the series solution only a finite number of terms have been included.

It is noted that in a practical analysis damping should be included and a longer time range may be considered as well.



$$\begin{aligned}
 R &= 67.115 \text{ in} \\
 h &= 1.0 \text{ in} \\
 b &= 1.0 \text{ in} \\
 \beta &= 15^\circ
 \end{aligned}
 \left. \vphantom{\begin{aligned} R \\ h \\ b \\ \beta \end{aligned}} \right\} \gamma = \beta^2 \frac{R}{h} = 4.6$$

$$H = 2.287 \text{ in}$$

TIME PARAMETER

$$\tau = \frac{C}{R} \times t$$

$$E = 10 \times 10^6 \text{ psi}$$

$$\nu = 0.2$$

$$P = 2.44 \times 10^{-4} \frac{\text{lb sec}^2}{\text{in}^4}$$

$$C = \sqrt{\frac{E}{P}} = 2.024 \times 10^5 \frac{\text{in}}{\text{sec}}$$

LOAD PARAMETER

$$P = \left(\frac{R^2}{h}\right) \times \frac{q}{E}$$

FIGURE 16 SIMPLY SUPPORTED SHALLOW ARCH

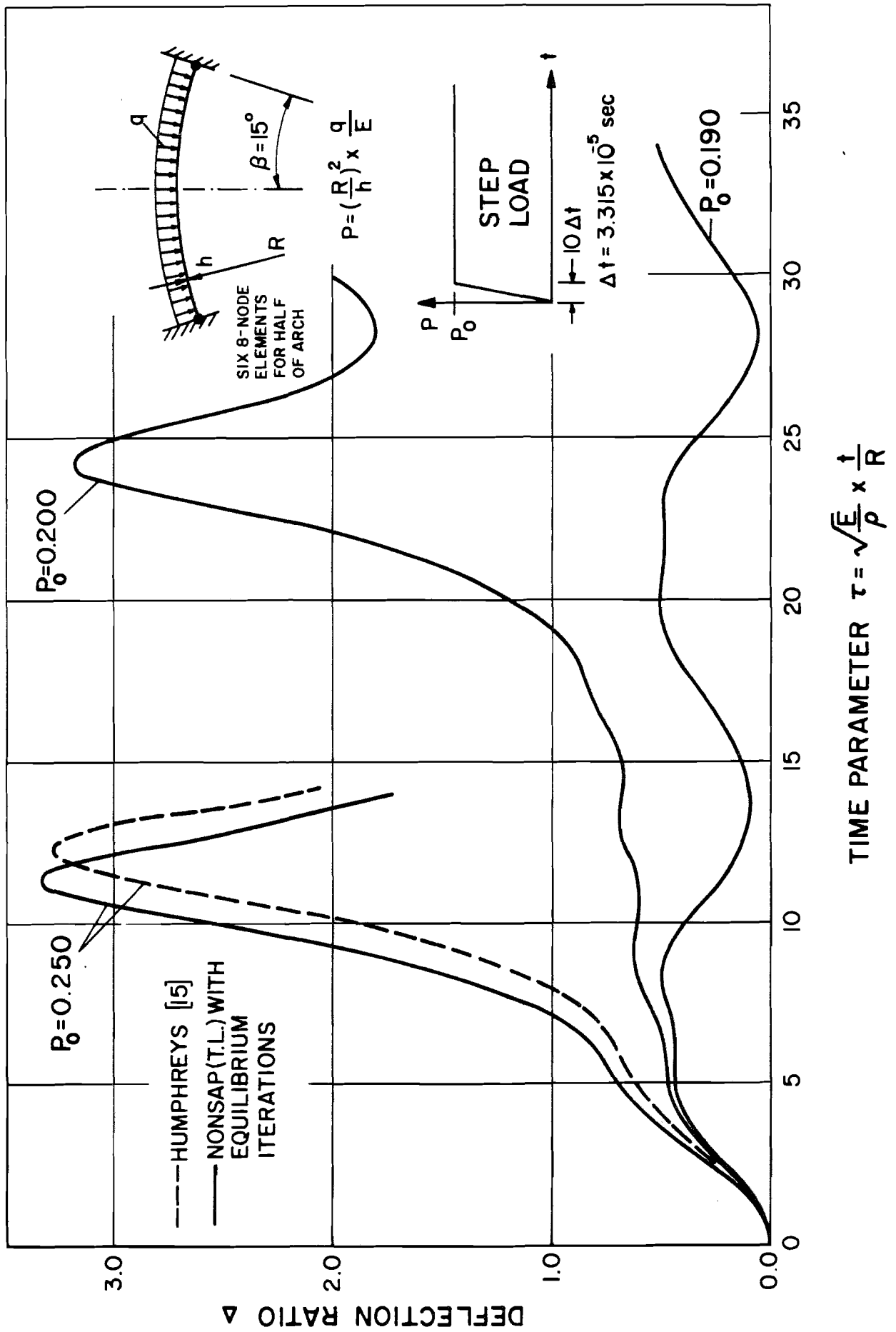


FIGURE 17 DYNAMIC SNAP-THROUGH OF A SHALLOW CIRCULAR ARCH

## 6. COMPARISON OF TOTAL LAGRANGIAN AND UPDATED LAGRANGIAN FORMULATIONS

An important observation, which was already stated earlier, is that both the T.L. and the U.L. formulations include all nonlinear effects due to large displacements, large strains and material nonlinearities. If the constitutive tensor is defined appropriately, as discussed in Section 3.4, the same numerical results are obtained. The only advantage of using one formulation rather than the other, is its better numerical efficiency.

It should be noted that the U.L. formulation is quite different from the moving coordinate formulation presented in the survey paper by Stricklin et al. [33], and the updated formulation, which was used in the comparative study by Dupuis et al. [5].

The incremental moving coordinate formulation presented by Stricklin et al. [33] was stated to be restricted to small strains and have distinct computational disadvantages. These conclusions do not apply to the U.L. formulation used in NONSAP.

The "updated" formulation employed by Dupuis et al. in their comparative study of this formulation versus a Lagrangian formulation, did not give satisfactory results [5]. However, using the U.L. formulation with isoparametric elements as presented in this report, the results are as good as obtained using the T.L. formulation. The only errors are due to the numerical solution of the governing continuum mechanics equations.

It should be noted that, in general, using both the T.L. and the U.L. formulations equilibrium iterations should be performed

in order to insure an accurate solution. If no equilibrium iterations are carried out, the linearization in each time step can introduce uncontrolled large errors. In the elastic and hyperelastic analyses presented here, it was possible to calculate the stresses in configuration 2 directly from the total strains, i.e. in the T.L. formulation total 2nd Piola-Kirchhoff stresses are obtained from total Green-Lagrange strains, and in the U.L. formulation total Cauchy stresses are obtained from total Almansi strains. Therefore, the nonlinear finite element equations have been solved "exactly" within the assumptions of the time integration scheme and the convergence limit of the iteration. In path dependent problems this is not possible and total stresses are calculated by adding increments in stresses (which, in the U.L. formulation, requires a transformation of  ${}^2S_{ij}$  in Eq. (16) to  ${}^2\tau_{ij}$ ).

The choice between the T.L. and U.L. formulations essentially depends on their relative numerical effectiveness. Table 1 shows that  ${}^1B_L$  is a full matrix whereas  ${}^1B_L$  is sparse, and that all other matrices of the two formulations have corresponding patterns of zero elements. The strain-displacement transformation matrix  ${}^1B_L$  is full because of the initial displacement effect in the linear strain terms, Eq. (11). Therefore, the calculation of the element matrices requires less time in the U.L. formulation.

An advantage of the T.L. formulation is that the derivatives of the interpolation functions are with respect to the initial configuration, and therefore need only be formed once, if they are stored on back-up storage for use in all load steps. However, in

practice, the use of tape or disc to store and retrieve the required derivatives in each step may be more costly than to simply recalculate them, and, in particular, the required storage is a problem size governing factor since saturation of back-up storage may be reached.

It appears that the choice for the T.L. or U.L. formulation will largely depend on the definition of the material constants, i.e. whether the constitutive law is given corresponding to the T.L. or the U.L. formulation. In reasonably small strain, elastic analysis the differences which arise by using the same material constants in both formulations--because, for instance, a clear definition of the constants may not be available--can be expected to be small (see Examples 2,3,5). In the analysis of hyperelastic materials the constitutive law is commonly defined corresponding to the T.L. formulation (see Example 4).

For (small and) large strain elastic-plastic analysis Hibbit et al. [13], Heifitz and Costantino [12] and Lee [20] suggest a definition of the material constants which lends itself to the use of the U.L. formulation. Heifitz and Costantino have actually used an updated formulation and analyzed metal forming problems in which up to 40% strains are measured. However, Hibbit et al. transformed the constitutive matrix established for the current configuration (configuration 1) to the initial configuration (configuration 0) in order to use the T.L. formulation.

Larsen suggests the use of the T.L. formulation and assumes that in large strain analysis increments in Kirchhoff stresses are related to increments in Green-Lagrange strains by essentially the

same constitutive matrix which is used in small strain elastic-plastic analysis [19]. However, he does not present solutions to large strain problems.

The use of the U.L. and the T.L. formulations for elastic-plastic analysis is currently under investigation and will be the subject of a separate report.

## CONCLUSIONS

The objective in this report was to present and compare the two general incremental formulations, which are used in the computer program NONSAP for nonlinear static and dynamic analysis. Both formulations have been derived from general principles of continuum mechanics and include material, large displacement and large strain nonlinearities.

The implementation of the formulations was discussed for elastic and hyperelastic materials only. Additional considerations are necessary in path dependent problems.

For the solution of problems in elasticity (and hyperelasticity) both formulations are, theoretically, equivalent and differences in results of analysis arise only due to different definition of the constitutive laws. The choice between the formulation is, therefore, only governed by their relative numerical efficiency discussed in the report.

To indicate the effectiveness of the solution procedures the analysis of large displacement static and dynamic buckling of arches and shells and the static and dynamic large strain response of a hyperelastic material was presented.

## REFERENCES

1. Argyris, J.H., Dunne, P.C., and Angelopoulos, T., "Nonlinear Oscillations Using the Finite Element Technique," *Computer Methods in Applied Mechanics and Engineering*, Vol. 2, pp. 203-250, 1973.
2. Bathe, K.J. and Wilson, E.L., "NONSAP--A General Finite Element Program for Nonlinear Dynamic Analysis of Complex Structures," Paper M3/1, Proceedings 2nd Int. Conference on Structural Mechanics in Reactor Technology, Berlin, September, 1973.
3. Bathe, K.J. and Wilson, E.L., "Stability and Accuracy Analysis of Direct Integration Methods," *International Journal of Earthquake Engineering and Structural Dynamics*, Vol. 1, pp. 283-291, 1973.
4. Belytschko, T., and Hsieh, B.J., "Nonlinear Transient Analysis of Shells and Solids of Revolution by Convected Elements," AIAA paper No. 73-359, AIAA/ASME/SAE 14th Structures, Structural Dynamics and Materials Conference, Williamsburg, Virginia, March, 1973.
5. Dupuis, G.A., Hibbitt, H.D., McNamara, S.F. and Marcal, P.V., "Nonlinear Material and Geometric Behavior of Shell Structures," *Computers and Structures*, Vol. 1, pp. 223-239, 1971.
6. Farhoomand, I., "Nonlinear Dynamic Stress Analysis of Two-Dimensional Solids," Ph.D. dissertation, University of California, Berkeley, 1970.
7. Felippa, C.A., "Refined Finite Element Analysis of Linear and Nonlinear Two-Dimensional Structures," SESM Report No. 66-22, Department of Civil Engineering, University of California, Berkeley, 1966.
8. Fung, Y.C., Foundations of Solid Mechanics, Prentice-Hall, Inc., Englewood Cliffs, New Jersey, 1965.
9. Gjelsvik, A. and Bodner, S.R., "The Energy Criterion and Snap Buckling of Arches." ASCE, *J. Engng. Mech. Div.*, Vol. 88, pp. 87-134, 1962.
10. Haug, E. and Powell, G.H., "Finite Element Analysis of Nonlinear Membrane Structures," SESM Report No. 72-7, Department of Civil Engineering, University of California, Berkeley, 1972.
11. Hartz, B.J. and Nathar, N.D., "Finite Element Formulation of Geometrically Nonlinear Problems of Elasticity," Recent Advances in Matrix Methods of Structural Analysis and Design, 1st Japan-U.S. Seminar on Matrix Methods of Structural Analysis and Design, University of Alabama Press, pp. 415-440, 1971.

12. Heifitz, J.H. and Costantino, C.J., "Dynamic Response of Nonlinear Media at Large Strains," ASCE, J. Engng. Mech. Div., Vol. 98, pp. 1511-1527, 1972.
13. Hibbitt, H.D., Marcal, P.V., and Rice, J.R., "Finite Element Formulation for Problems of Large Strain and Large Displacements," Int. J. Solids Struct., Vol. 6, pp. 1069-1086, 1970.
14. Holden, J.T., "On the Finite Deflections of Thin Beams," Int. J. Solids Struct., Vol. 8, pp. 1051-1055, 1972.
15. Humphreys, J.S., "On Dynamic Snap Buckling of Shallow Arches," AIAA Journal, Vol. 4, pp. 878-886, 1966.
16. Iding, R.H., "Identification of Nonlinear Materials by Finite Element Methods," SESM Report No. 73-4, Department of Civil Engineering, University of California, Berkeley, 1973.
17. Jensen, P.S., "Transient Analysis of Structures by Stiffly Stable Methods," Computers and Structures, to appear.
18. Kornishin, H.S. and Isanbaeva, F.S., "Flexible Plates and Panels," (in Russian), Nauka, Moscow, 1968.
19. Larsen, P.K., "Large Displacement Analysis of Shells of Revolution, including Creep, Plasticity and Viscoelasticity," SESM Report No. 71-22, Department of Civil Engineering, University of California, Berkeley, 1971.
20. Lee, E.H., "Elastic-Plastic Deformation at Finite Strains," Transactions of the ASME, Journal of Applied Mechanics, March, 1968.
21. Mallet, R.H., and Berke, L., "Automated Method for the Large Deflection and Instability Analysis of 3-Dimensional Truss and Frame Assemblies," AFFDL-TR-66-102, December, 1966.
22. Malvern, L.E., Introduction to the Mechanics of a Continuous Medium, Prentice-Hall, Inc., Englewood Cliffs, New Jersey, 1969.
23. Marcal, P.V., "The Effect of Initial Displacements on Problems of Large Deflection and Stability," Report of Brown University, Division of Engineering, 1967.
24. Murray, D.W. and Wilson, E.L., "Finite Element Large Deflection Analysis of Plates," ASCE, J. Eng. Mech. Div., Vol. 95, Feb., 1969.
25. McNamara, J.F., "Incremental Stiffness Method for Finite Element Analysis of the Nonlinear Dynamic Problem," Ph.D. thesis, Department of Civil Engineering, Brown University, 1972.
26. Nickell, R.E., "Direct Integration Methods in Structural Dynamics," ASCE, J. Engng. Mech. Div., Vol. 99, pp. 303-317, 1973.

27. Oden, J.T., "Finite Element Applications in Nonlinear Structural Analysis," Proc. of the Symposium on "Application of Finite Element Methods in Civil Engineering," Nashville, Tenn., Nov., 1969.
28. Oden, J.T., Finite Elements of Nonlinear Continua, McGraw-Hill, 1972.
29. Schreyer, H. and Masur, E., "Buckling of Shallow Arches," ASCE, J. Engng. Mech. Div., Vol. 92, pp. 1-19, 1966.
30. Sharifi, P. and Popov, E.P., "Nonlinear Buckling Analysis of Sandwich Arches," ASCE, J. Engng. Mech. Div., pp. 1397-1412, 1970.
31. Sharifi, P. and Yates, D.N., "Nonlinear Thermo-Elastic-Plastic and Creep Analysis by the Finite Element Method," AIAA Paper No. 73-358, AIAA/ASME/SAE 14th Structures, Structural Dynamics and Materials Conference, Williamsburg, Virginia, March, 1973.
32. Stricklin, J.A., "Geometrically Nonlinear Static and Dynamic Analysis of Shells of Revolution," High Speed Computing of Elastic Structures, Proceedings of the Symposium of IUTAM, Univ. of Liege, pp. 383-411.
33. Stricklin, J.A., Von Riesenmann, W.A., Tillerson, J.R. and Haisler, W.E., "Static Geometric and Material Nonlinear Analysis," Advances in Computational Methods in Structural Mechanics and Design, 2nd U.S.-Japan Seminar on Matrix Methods of Structural Analysis and Design, University of Alabama Press, 1972, pp. 301-324.
34. Yaghmai, S., "Incremental Analysis of Large Deformations in Mechanics of Solids with Applications to Axisymmetric Shells of Revolution," SESM Report No. 69-17, Department of Civil Engineering, University of California, Berkeley, 1968.
35. Yaghmai, S. and Popov, E.P., "Incremental Analysis of Large Deflections of Shells of Revolution," Int. J. of Solids and Struct., Vol. 7, pp. 1375-1393, 1971.
36. Yamada, Y., "Incremental Formulation for Problems with Geometric and Material Nonlinearities," Advances in Computational Methods in Structural Mechanics and Design, 2nd U.S.-Japan Seminar on Matrix Methods of Structural Analysis and Design, University of Alabama Press, pp. 325-355, 1972.
37. Yeh, C.H., "Large Deflection Dynamic Analysis of Thin Shells Using the Finite Element Method," SESM Report No. 70-78, Department of Civil Engineering, University of California, 1970.
38. Zienkiewicz, O.C., The Finite Element Method in Engineering Science, McGraw-Hill, London, 1971.

APPENDIX A

DERIVATION OF THE INCREMENTAL STRESS-STRAIN MATRIX  
FOR HYPERELASTIC INCOMPRESSIBLE MATERIAL (PLANE STRESS)

In plane stress analysis the constitutive relation for a hyper-elastic incompressible isotropic material can be expressed as [16]

$$\begin{bmatrix} {}^1_0 S_{11} \\ {}^1_0 S_{22} \\ {}^1_0 S_{12} \end{bmatrix} = 2C_1 \left\{ \begin{bmatrix} 1 \\ 1 \\ 0 \end{bmatrix} - \mu^2 \begin{bmatrix} C_{22} \\ C_{11} \\ -C_{12} \end{bmatrix} \right\} + 2C_2 \left\{ \mu \begin{bmatrix} 1 \\ 1 \\ 0 \end{bmatrix} + [1-\mu^2(C_{11} + C_{22})] \begin{bmatrix} C_{22} \\ C_{11} \\ -C_{12} \end{bmatrix} \right\} \quad (A1)$$

where the plane stress condition  ${}^1_0 S_{33} = 0$  has already been used to eliminate the hydrostatic pressure. Further the incompressibility condition

$$\mu [C_{11}C_{22} - (C_{12})^2] = 1 \quad (A2)$$

has to be satisfied. In Eqs. (A1) and (A2)

$$\begin{aligned} {}^1_0 S_{ij} &= \text{components of the 2nd Piola-Kirchhoff stress tensor} \\ C_{ij} = 2 {}^1_0 \epsilon_{ij} + \delta_{ij} &= \text{components of the deformation tensor related to the Lagrange strain tensor} \\ &\quad {}^1_0 \epsilon_{ij}, \delta_{ij} = \text{Kronecker delta} \\ \mu = C_{33} &= \text{deformation measure normal to the plane} \\ C_1, C_2 &= \text{material functions defined by } C_i = \frac{\partial W}{\partial I_i} \\ &\quad (W = \text{strain energy function} \\ &\quad \quad I_i = \text{strain invariants}) \end{aligned}$$

The following expression for the strain energy function  $W$  can be assumed for some rubber like materials

$$W = C_1(I_1 - 3) + C_2(I_2 - 3) \quad (A3)$$

where  $C_1$  and  $C_2$  are constants.

For the incremental T.L. formulation the required stress-strain matrix  ${}_o C$  defined by

$$\begin{bmatrix} {}_o S_{11} \\ {}_o S_{22} \\ {}_o S_{12} \end{bmatrix} = {}_o C \begin{bmatrix} {}_o \epsilon_{11} \\ {}_o \epsilon_{22} \\ 2 {}_o \epsilon_{12} \end{bmatrix} \quad (A4)$$

is found by forming the gradient of Eq. (A1), i.e.

$${}_o C_{ijkl} = \frac{\partial {}_o^1 S_{ij}}{\partial {}_o^1 \epsilon_{kl}} \quad (A5)$$

(Note that first Eq. (A2) is used to eliminate the additional unknown  $\mu$ .) This leads to

$$\begin{aligned} {}_o C = & 4 C_1 \mu^2 \left\{ 2\mu C + \begin{bmatrix} 0 & -1 & 0 \\ -1 & 0 & 0 \\ 0 & 0 & +1 \end{bmatrix} \right\} \\ & + 4 C_2 \mu^2 \left\{ 2\mu (C_{11} + C_{22}) C + (C_{11} + C_{22}) \begin{bmatrix} 0 & -2 & 0 \\ -2 & 0 & 0 \\ 0 & 0 & 0.5 \end{bmatrix} \right. \\ & \left. + \begin{bmatrix} -2C_{22} & \frac{1}{\mu^2} & C_{12} \\ \frac{1}{\mu^2} & -2C_{11} & C_{12} \\ C_{12} & C_{12} & -\frac{1}{2\mu^2} \end{bmatrix} \right\} \quad (A6) \end{aligned}$$

where

$$C = \begin{bmatrix} (C_{22})^2 & C_{11}C_{22} & -C_{12}C_{22} \\ & (C_{11})^2 & -C_{12}C_{11} \\ \text{symmetric} & & (C_{12})^2 \end{bmatrix} \quad (A7)$$

In other than plane stress analysis the hydrostatic pressure cannot be eliminated, and has to be included as an additional variable. The incompressibility condition yields the additional equations for the unknown hydrostatic pressure.